SUPPORTING INFORMATION

Heterotropic Cooperativity within and between Protomers of an Oligomeric M_2 Muscarinic Receptor

Rabindra V. Shivnaraine,[†] Xi-Ping Huang,[‡] Margaret Seidenberg,[‡] John Ellis,[‡] and James W. Wells[†]

[†]*Department of Pharmaceutical Sciences, Leslie Dan Faculty of Pharmacy, University of Toronto, Toronto, Ontario M5S 3M2.*
[‡]*Departments of Psychiatry and Pharmacology, Hershey Medical Center, Penn State University College of Medicine, Hershey, PA 17033.*

MODES OF COOPERATIVITY WITHIN AN OLIGOMER

G protein-coupled receptors for biogenic amines bind agonists at an orthosteric site located within the cluster of transmembrane helices (*1*). Muscarinic cholinergic receptors also contain an allosteric site at the extracellular surface between loops 2 and 3 (*2,3*) (Figure S1). Antagonists such as *N*-[^{3}H]methyl-scopolamine (NMS) and [^{3}H]quinuclidinylbenzilate (QNB) bind exclusively to the orthosteric site at the concentrations used in binding assays (*1*), and compounds such as gallamine bind to the allosteric site (*3*).

A monomer of the receptor can exhibit one mode of cooperativity: namely, intramolecular heterotropic cooperativity between an allosteric ligand and an orthosteric ligand (Figure S1A). A dimer or larger oligomer can exhibit three additional modes not possible in a monomer: intermolecular homotropic cooperativity between two or more allosteric ligands (Figure S1B), intermolecular homotropic cooperativity between two or more orthosteric ligands (Figure S1C), and intermolecular heterotropic cooperativity between an allosteric ligand on one protomer and an orthosteric ligand on another (Figure S1D). In a system at thermodynamic equilibrium, a monomer will yield a Hill coefficient of 1 for the binding of either ligand taken alone or in the presence of the other; a dimer or larger oligomer can yield more complex patterns (*4*).

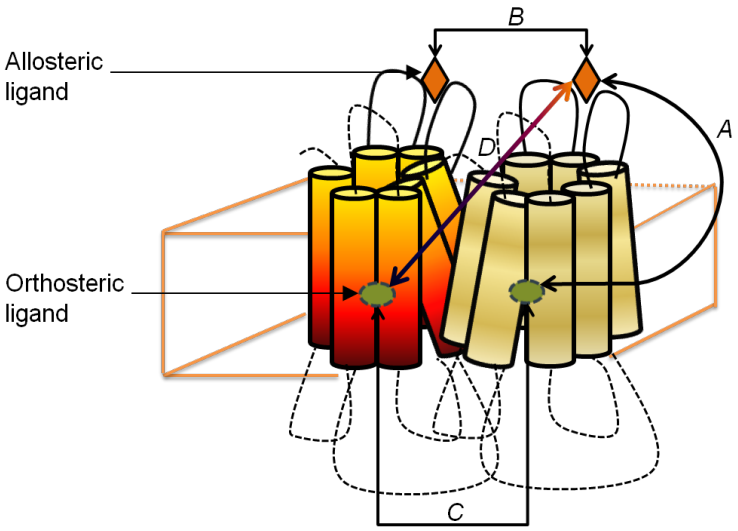

Figure S1. Modes of cooperativity between orthosteric and allosteric sites within a dimer. (A) Intramolecular heterotropic cooperativity. (B) Homotropic cooperativity between allosteric sites. (C) Homotropic cooperativity between orthosteric sites. (D) Inter-molecular heterotropic cooperativity.

KINETICALLY DETERMINED MODELS OF BINDING

Two cooperative systems were examined for the effects of occupancy and the order of mixing on the time-course of binding: a monomeric receptor with one allosteric and one orthosteric site, and a dimeric receptor with one allosteric site and one orthosteric site per protomer. Each system included one allosteric ligand (A) and one orthosteric ligand (L), and the level of each species of receptor over time was computed by numerical integration of the corresponding differential equations. There was no differential equation for either ligand, the free concentration of which was taken as known. It therefore was assumed that neither was depleted through binding to the receptor. The simulations were performed in MATLAB 2008a, and the integrals were calculated using the ODE23s subroutine. The latter is an implementation of a modified Rosenbrock formula of order 2, in which the Rosenbrock method is modified by a second-order Wolfbrandt formula (*5*).

Monomeric Receptor. A receptor (R) binds an allosteric ligand (A) and an orthosteric ligand (L) at topographically distinct sites as depicted in Scheme 2, reproduced below from the parent text. The receptor may bind one equivalent of either ligand alone, forming a binary complex (AR or RL), or one equivalent of each, forming a ternary complex (ARL).

SCHEME 2

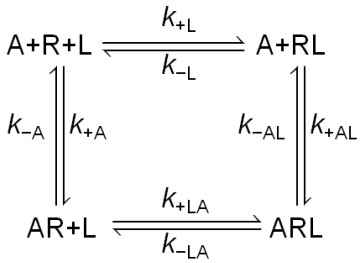

The parameters k_{-L} and k_{+L} are the first- and second-order rate constants for the binding of L to R; similarly, k_{-A} and k_{+A} are the first- and second-order rate constants for the binding of A to R. The parameters k_{-LA} and k_{+LA} are the corresponding rate constants for the binding of L to AR, and k_{-AL} and k_{+AL} are those for the binding of A to RL. The rate constants and corresponding equilibrium dissociation constants (K) are related according to Equations S1–S4, where the cooperativity factor α ensures that all values are consistent with the principle of microscopic reversibility.

$$K_{\mathrm{L}} = \frac{[\mathrm{R}][\mathrm{L}]}{[\mathrm{RL}]} \equiv \frac{k_{-\mathrm{L}}}{k_{+\mathrm{L}}} \tag{S1}$$

$$K_{\mathrm{A}} = \frac{[\mathrm{A}][\mathrm{R}]}{[\mathrm{AR}]} \equiv \frac{k_{-\mathrm{A}}}{k_{+\mathrm{A}}} \tag{S2}$$

$$K_{\mathrm{LA}} = \frac{[\mathrm{AR}][\mathrm{L}]}{[\mathrm{ARL}]} \equiv \frac{k_{-\mathrm{LA}}}{k_{+\mathrm{LA}}} \equiv \alpha K_{\mathrm{L}} \tag{S3}$$

$$K_{\mathrm{AL}} = \frac{[\mathrm{A}][\mathrm{RL}]}{[\mathrm{ARL}]} \equiv \frac{k_{-\mathrm{AL}}}{k_{+\mathrm{AL}}} \equiv \alpha K_{\mathrm{A}} \tag{S4}$$

In a system observed at thermodynamic equilibrium, the unique effect of the cooperativity factor α is to establish the equilibrium dissociation constant of L in the presence of A (*i.e.*, αK_{L}) and *vice versa* (*i.e.*, αK_{A}). In a kinetically determined system, α may affect either or both of the constituent rate constants according to Equations S5 and S6, in which the balance is established by the value of j.

$$\frac{k_{-\mathrm{LA}}}{k_{+\mathrm{LA}}} = \alpha\frac{k_{-\mathrm{L}}}{k_{+\mathrm{L}}} \equiv \frac{\alpha^{j+1}k_{-\mathrm{L}}}{\alpha^{j}k_{+\mathrm{L}}} \equiv \frac{\left(\frac{1}{\alpha}\right)^{j}k_{-\mathrm{L}}}{\left(\frac{1}{\alpha}\right)^{j+1}k_{+\mathrm{L}}} \tag{S5}$$

$$\frac{k_{-\mathrm{AL}}}{k_{+\mathrm{AL}}} = \alpha\frac{k_{-\mathrm{A}}}{k_{+\mathrm{A}}} \equiv \frac{\alpha^{j+1}k_{-\mathrm{A}}}{\alpha^{j}k_{+\mathrm{A}}} \equiv \frac{\left(\frac{1}{\alpha}\right)^{j}k_{-\mathrm{A}}}{\left(\frac{1}{\alpha}\right)^{j+1}k_{+\mathrm{A}}} \tag{S6}$$

When $j \geq 1$, the cooperative effect of one ligand on the binding of another is partitioned between the rates of dissociation and association according to the arbitrary ratio α^{j+1}/α^{j}. When $j = 0$, the cooperative effect of L on the binding of A is assigned exclusively to the rate of dissociation or association of the allosteric ligand (*i.e.*, $\frac{k_{-\mathrm{AL}}}{k_{+\mathrm{AL}}} = \frac{\alpha k_{-\mathrm{A}}}{k_{+\mathrm{A}}}$ or $\frac{k_{-\mathrm{AL}}}{k_{+\mathrm{AL}}} = \frac{k_{-\mathrm{A}}}{(1/\alpha)k_{+\mathrm{A}}}$); similarly, the cooperative effect of A on the binding of L is assigned exclusively to the rate of dissociation or association of the orthosteric ligand (*i.e.*, $\frac{k_{-\mathrm{LA}}}{k_{+\mathrm{LA}}} = \frac{\alpha k_{-\mathrm{L}}}{k_{+\mathrm{L}}}$ or $\frac{k_{-\mathrm{LA}}}{k_{+\mathrm{LA}}} = \frac{k_{-\mathrm{L}}}{(1/\alpha)k_{+\mathrm{L}}}$).

The assumption that α and j are the sole determinants of changes in the first- and second-order rate constants leads to Equations S7–S10, which were used to calculate the rate constants for simulations in terms of Scheme 2. The values of j were chosen to yield parametric values that approximate those reported for gallamine and *N*-methylscopolamine at the M_2 muscarinic receptor.

$$k_{-\mathrm{LA}} = \left(\frac{1}{\alpha}\right)^{2}k_{-\mathrm{L}} \tag{S7}$$

$$k_{-\mathrm{AL}} = \left(\frac{1}{\alpha}\right)^{0}k_{-\mathrm{A}} \tag{S8}$$

$$k_{+\mathrm{LA}} = \left(\frac{1}{\alpha}\right)^{3}k_{+\mathrm{L}} \tag{S9}$$

$$k_{+\mathrm{AL}} = \left(\frac{1}{\alpha}\right)^{1}k_{+\mathrm{A}} \tag{S10}$$

The kinetically determined description of Scheme 2 comprises four differential equations, one for each species of receptor (*i.e.*, R, AR, RL, and ARL). The time-course for the appearance or loss of each species was computed for three initial conditions that correspond to three experimental protocols: simultaneous addition of A and L to R, premixing of A and R followed by the addition of L, and premixing of L and R followed by the addition of A. The values of $k_{-\mathrm{A}}$, K_{A}, $k_{-\mathrm{L}}$, K_{L}, and α were taken as measured for gallamine and *N*-[^{3}H]methylscopolamine, and those of $k_{+\mathrm{A}}$, $k_{+\mathrm{L}}$, $k_{\pm\mathrm{AL}}$, and $k_{\pm\mathrm{LA}}$ were calculated according to Equations S1–S10.

Data simulated according to Scheme 2 are shown in Figure S16, and the values of all parameters are listed in Table S12. In the absence of cooperativity ($\alpha = 1$), the value of the apparent first-order rate constant (k_{obsd}) for the appearance of total bound L (*i.e.*, [RL] + [ARL]) in the presence of 10 nM A is 0.40 min^{-1}; the concentration of L equals its equilibrium dissociation constant (10 nM), and the level of occupancy by L at equilibrium therefore is 50% (Figure S16A). When binding is cooperative ($\alpha = 46$) under otherwise identical conditions, the value of k_{obsd} is reduced to 0.24 min^{-1} irrespective of whether A precedes L, A and L are added simultaneously, or L precedes A; the affinities are reduced 46-fold, and the level of occupancy by L at equilibrium is 23% (Figure S16B–D). The rate at which total binding of the orthosteric ligand attains equilibrium therefore is independent of the order in which the allosteric and

orthosteric ligands are added to the receptor. The same result is obtained at higher concentrations of A, albeit more slowly (*e.g.*, k_{obsd} = 0.040 min^{-1} when [A] = 1.0 μM).

A special case of Scheme 2 is shown below as Scheme S1, in which pathways to and from the ternary complex via AR are disallowed (*i.e.*, $k_{+LA} = 0$ and $k_{-LA} = 0$). Access of L to and from the orthosteric site therefore can occur only via RL, in which the allosteric site is vacant. Scheme S1 has been used to rationalize the effect of alcuronium on the binding of *N*-[^{3}H]methylscopolamine to muscarinic receptor in membranes from rat atria, where the allosteric ligand appeared to obstruct passage of the radioligand to and from the orthosteric site (*6*).

SCHEME S1

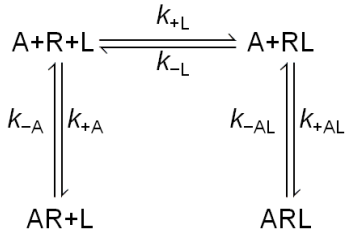

Data were simulated according to Scheme S1 for the three sets of initial conditions described above. The concentration of L (10 nM) and the parametric values were the same as those used in the simulations according to Scheme 2 (Table S12), except for the absent parameters k_{+LA} and k_{-LA}, and the concentration of A was set at different values from 10 nM to 100 μM. The data obtained with the concentration of A set at 10 nM are shown in Figure S17. The apparent rate constants (k_{obsd}) for the best fits of a single exponential to the traces for total bound L (*i.e.*, [RL] + [ARL]) at all concentrations of A are listed in Table S13.

In contrast to Scheme 2, the rate at which the system approaches equilibrium in Scheme S1 varies with the order in which the two ligands are added to the receptor (Table S13). When A precedes L, the system equilibrates more slowly than it does when both ligands are added together. When L precedes A, the relative rate of equilibration depends upon the concentration of the allosteric ligand. At lower concentrations of A, equilibration is slower than it is when both ligands are added together; at higher concentrations of A, equilibration is faster than it is when both ligands are added together. The differences are determined by the rate of association of the allosteric ligand with vacant R. At high concentrations of A, the value of k_{+A}[A] is large, and receptors are directed toward the formation of AR (*i.e.*, A + R + L ⇌ AR + L), That in turn slows the formation of ARL. Schemes 2 and S1 are equivalent at thermodynamic equilibrium owing to the requirement for reciprocity in the effect of A on the binding of L and *vice versa*. Both models therefore predict that the asymptotic level of occupancy by L is 23% (cf. Figures S16B–D and Figures S17A–C).

Dimeric Receptor. Each protomer (j) of a homodimer contains one orthosteric site (L_j) and one allosteric site (A_j) as illustrated in Figure S2 (j = 1 or 2). In principle, an oligomeric array might be symmetric or asymmetric with respect to the binding of a ligand to homologous sites on constituent protomers. In a symmetric array, all vacant sites are of equal affinity for the ligand; in an asymmetric array, vacant sites differ in their affinity for the ligand, presumably as a consequence of conformational restraints within the oligomer. In either arrangement, homotropic cooperativity may create or augment differences in affinity between one equivalent of ligand and the next. It is assumed here that the vacant dimer is symmetric with respect to both ligands, and the microscopic equilibrium dissociation constant for the binding of ligand L to either orthosteric site is therefore K_L (Equation S1); similarly, the dissociation constant for the binding of ligand A to either allosteric site is K_A (Equation S2).

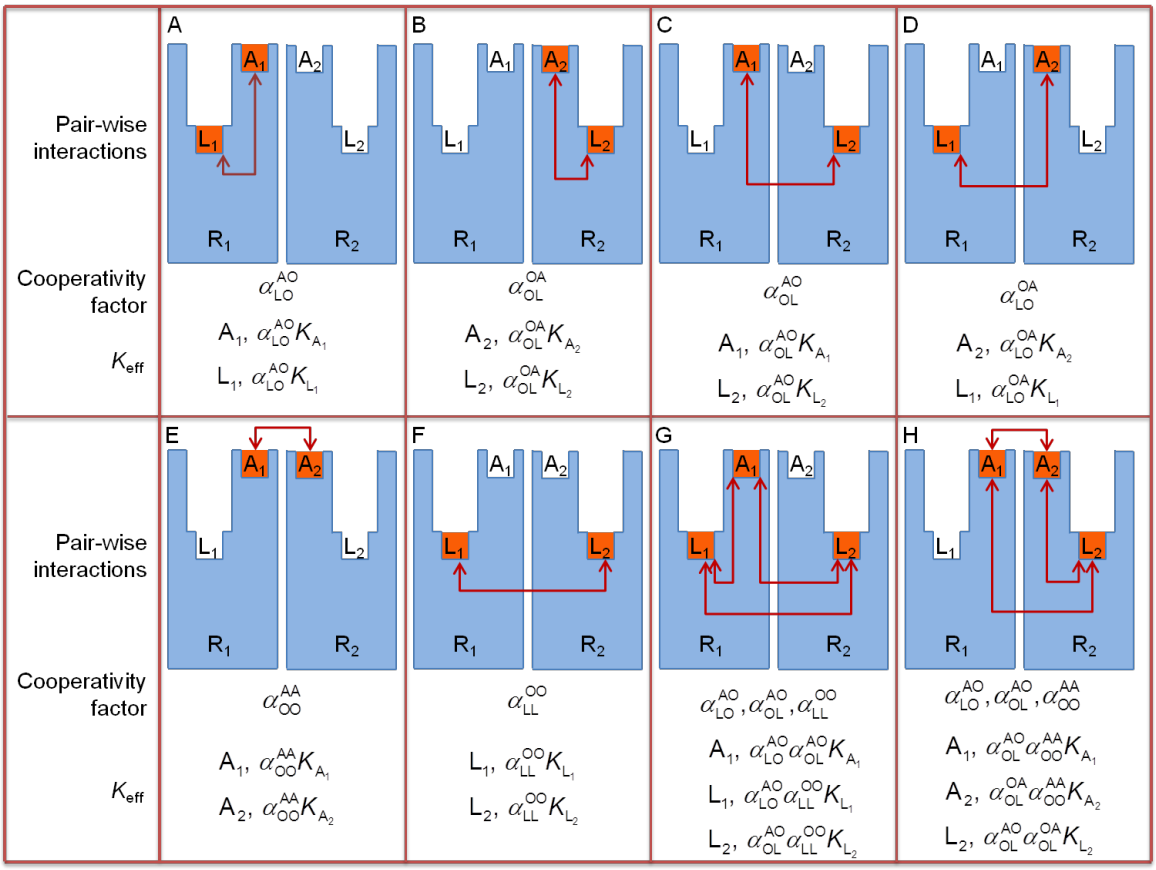

Figure S2. Modes of cooperativity within a dimer. The protomers of the dimer are shown as R_1 and R_2. Within each protomer, the allosteric and orthosteric sites are shown as A_1 and L_1 (Protomer 1) or A_2 and L_2 (Protomer 2). Vacant sites are unfilled, and occupied sites are colored orange. Cooperativity factors are designated α and qualified as to the identity of the relevant sites as allosteric (superscript) or orthosteric (subscript); each site is identified as vacant (O) or occupied by the corresponding ligand (A or L). The microscopic equilibrium dissociation constant for the binding of L or A to protomer j is shown as K_{Lj} or K_{Aj}, respectively. The two protomers were taken as equivalent in the simulations presented in Figure 10 and Table S15 (*e.g.*, $K_{L1} = K_{L2}$). A different liganded state of the dimer is depicted in each panel, and the arrows indicate the paired interactions between specific ligands. Also shown are the corresponding cooperativity factors and the equilibrium dissociation constant (K_{eff}) for each equivalent of ligand. panels A–F. Complexes with a single cooperative interaction. panels G and H. Complexes with three cooperative interactions.

Additional equivalents of either ligand bind with affinities that are the product of K_L or K_A and one or more cooperativity factors (α), the values of which are determined by the status of neighboring sites (Figure S2). Cooperativity factors can be homotropic (*i.e.*, α_{LL}^{OO}, α_{OO}^{AA}) or heterotropic (*i.e.*, α_{LO}^{AO}, α_{OL}^{OA}, α_{OL}^{AO}, α_{LO}^{OA}), and the latter can be intramolecular (α_{LO}^{AO}, α_{OL}^{OA}) or intermolecular (α_{OL}^{AO}, α_{LO}^{OA}). The affinity of A for the allosteric site of an L-bearing protomer within an otherwise vacant dimer is therefore $\alpha_{LO}^{AO}K_A$ (Figure S2A) or $\alpha_{OL}^{OA}K_A$ (Figure S2B); likewise, the affinity of L for the orthosteric site of an A-bearing protomer is $\alpha_{LO}^{AO}K_L$ or $\alpha_{OL}^{OA}K_L$. The affinity of A for the allosteric site of an otherwise vacant protomer adjacent to an L-bearing protomer is $\alpha_{OL}^{AO}K_A$ (Figure S2C) or $\alpha_{LO}^{OA}K_A$ (Figure S2D), and the

corresponding affinity of L is $\alpha_{OL}^{AO}K_L$ or $\alpha_{LO}^{OA}K_L$. The affinity of a second equivalent of A or L for an otherwise vacant dimer is $\alpha_{OO}^{AA}K_A$ (Figure S2E) or $\alpha_{LL}^{OO}K_L$ (Figure S2F), respectively.

At higher levels of occupancy, the overall or macroscopic cooperativity factor for the interaction between ligands at any two sites is the product of the cooperativity factors for all pair-wise interactions within the complex. In a triliganded dimer with one equivalent of A and two equivalents of L (Figure S2G), for example, the affinity of A for allosteric site A_1 is $\alpha_{LO}^{AO}\alpha_{OL}^{AO}K_A$ (Figure S2G); the corresponding affinity of L for orthosteric site L_1 is $\alpha_{LO}^{AO}\alpha_{LL}^{OO}K_L$, and that for orthosteric site L_2 is $\alpha_{OL}^{AO}\alpha_{LL}^{OO}K_L$. In a dimer with one equivalent of L and two equivalents of A (Figure S2H), the affinity of L for orthosteric site L_2 is $\alpha_{OL}^{AO}\alpha_{OL}^{OA}K_L$; the corresponding affinity of A for allosteric site A_1 is $\alpha_{OL}^{AO}\alpha_{OO}^{AA}K_A$, and that for allosteric site A_2 is $\alpha_{OL}^{OA}\alpha_{OO}^{AA}K_A$.

Extending the notion of symmetry, the degree of intra- or intermolecular cooperativity at each level of occupancy is assumed to be independent of the configuration of ligands within the dimer (*e.g.*, $\alpha_{LO}^{AO} = \alpha_{OL}^{OA}$ and $\alpha_{OL}^{AO} = \alpha_{LO}^{OA}$, but $\alpha_{LO}^{AO} \neq \alpha_{OL}^{AO}$); similarly, homotropic cooperativity between allosteric or orthosteric sites is assumed to be independent of heterotropic cooperativity (*i.e.*, $\alpha_{OO}^{AA} = \alpha_{LO}^{AA} = \alpha_{LL}^{AA}$ and $\alpha_{LL}^{OO} = \alpha_{LL}^{AO} = \alpha_{LL}^{AA}$). Also, the oligomeric status of the receptor is taken as constant; that is, there is no exchange of subunits within the system, although the model can accommodate processes in which dissociated monomers regroup without exchanging partners. Finally, pharmacological selectivity is assumed to be absolute: the allosteric ligand does not bind to the orthosteric site, and the orthosteric ligand does not bind to the allosteric site.

All possible species of a dimer in the presence of one allosteric ligand and one orthosteric ligand are shown in Scheme 3, reproduced below from the parent text. The dimer is designated as R, and the state of occupancy is indicated in the manner described for the cooperativity factors (Figure S2). Sites may be allosteric (superscipt) or orthosteric (subscript), and a site can be vacant (O) or occupied by the relevant ligand (A or L). Vacant dimers therefore are depicted as R_{OO}^{OO}, where the first position of the superscript or subscript denotes protomer 1 and the second position denotes protomer 2; similarly, fully occupied dimers are depicted as R_{LL}^{AA}. Occupancy by the allosteric ligand alone (R_{OO}^{OA}, R_{OO}^{AO}, R_{OO}^{AA}), the orthosteric ligand alone (R_{OL}^{OO}, R_{LO}^{OO}, and R_{LL}^{OO}), and combinations of both ligands are depicted in an analogous manner.

SCHEME 3

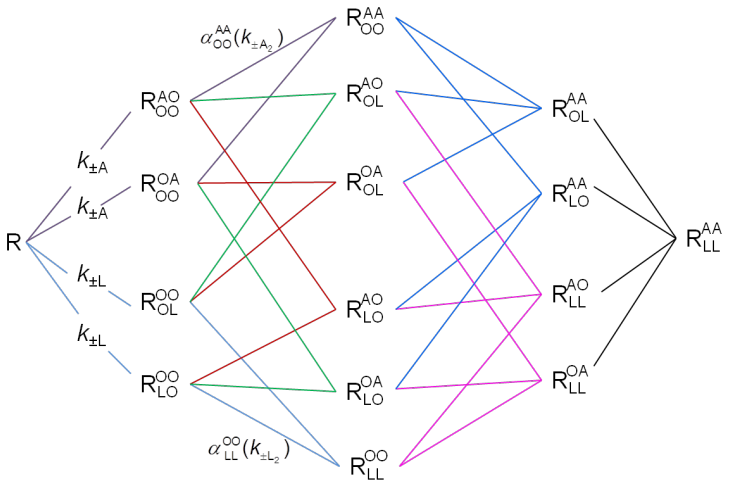

The kinetically determined description of Scheme 3 comprises 16 differential equations, one for each species of receptor, and 64 rate constants. In accord with the assumption of symmetry, the first- and second-order rate constants for the binding of A or L to either protomer of a vacant receptor are k_{-A} and k_{+A} or k_{-L} and k_{+L}, respectively. Following the approach described above for Scheme 2, the values of k_{+A} and k_{+L} were calculated from arbitrary values of k_{-A}, k_{-L}, K_A, and K_L (Equations S1 and S2). These four rate constants and the cooperativity factors α_{OO}^{AA}, α_{LL}^{OO}, $\alpha_{LO}^{AO} = \alpha_{OL}^{OA}$, and $\alpha_{LO}^{OA} = \alpha_{OL}^{AO}$ were used in turn to compute the remaining 60 rate constants for the binding of a second, third, or fourth equivalent of ligand.

Rate constants for an additional ligand were calculated according to equations of the form $k_{-X(Y)} = \left(\frac{1}{\Pi\alpha}\right)^{j} k_{-X}$ or $k_{+X(Y)} = \left(\frac{1}{\Pi\alpha}\right)^{j+1} k_{+X}$, where X denotes the ligand (*i.e.*, A or L), Y describes the state of occupancy in the absence of X (*i.e.*, AL, AAL, or ALL), and $\Pi\alpha$ is the product of all cooperativity factors as shown in Figure S2. Taken together, Y and $\Pi\alpha$ control the various pair-wise interactions that determine binding. For example, the rate constants for the binding of L at site L_1 of the species R_{OL}^{AO} are given by Equations S11 and S12 (Figure S2G).

$$k_{-L(AL)} = \left(\frac{1}{\alpha_{LO}^{AO}}\right)^{j} \left(\frac{1}{\alpha_{LL}^{OO}}\right)^{j} k_{-L} \tag{S11}$$

$$k_{+L(AL)} = \left(\frac{1}{\alpha_{LO}^{AO}}\right)^{j+1} \left(\frac{1}{\alpha_{LL}^{OO}}\right)^{j+1} k_{+L} \tag{S12}$$

Similarly, the rate constants for the binding of A at site A_1 of the species R_{OL}^{OA} are given by Equations S13 and S14 (Figure S2H).

$$k_{-A(AL)} = \left(\frac{1}{\alpha_{OL}^{AO}}\right)^{j} \left(\frac{1}{\alpha_{OO}^{AA}}\right)^{j} k_{-A} \tag{S13}$$

$$k_{+A(AL)} = \left(\frac{1}{\alpha_{OL}^{AO}}\right)^{j+1} \left(\frac{1}{\alpha_{OO}^{AA}}\right)^{j+1} k_{+A} \tag{S14}$$

In Equations S11 and S12, or in Equations S13 and S14, the relevant cooperativity factors are partitioned between the rates of association and dissociation according to the ratio $(1/\alpha)^{j}/(1/\alpha)^{j+1}$ as described above (cf. Equations S5 and S6). Values of α and j were selected to avoid rate constants that exceeded the diffusion limit, taken as 9.6×10^{10} $M^{-1}min^{-1}$; the latter was calculated according to the expression $(4RT)/(3\pi\eta)$ for a system at 297 K with the viscosity of water (η) (*7*).

Simulations in terms of Scheme 3 are illustrated in Figure 10 of the parent text, and the parametric values are listed in part in Table S14. The latter were chosen to mimic the arrangement proposed in Figure 9. Thus, heterotropic cooperativity slowed the reaction in both directions but in a disproportionate manner that depended upon the locations of the interacting sites within the dimer. Whereas cooperativity between allosteric and orthosteric sites on adjacent protomers was positive, that between sites on the same

protomer was negative. The parametric values obtained from analyses of the simulated data according to Equation 3 are listed in Table S15.

The result of this arrangement is a bell-shaped binding pattern in which positive heterotropic cooperativity leads to an increase in bound L at lower concentrations of A and negative heterotropic cooperativity leads to a decrease in bound L at higher concentrations (Figure 10). A time-dependent increase in the amplitude of the peak at intermediate concentrations of A is accompanied by a slower increase in the asymptote at saturating concentrations (Figure 10A). The simulated data therefore resemble the binding patterns obtained in experiments on the solubilized receptor at different times prior to equilibrium, particularly at intermediate and high concentrations of gallamine (Figures 2 and 3).

To mimic the effect of gallamine at different concentrations of *N*-[^{3}H]methylscopolamine, integration was continued until the system had attained equilibrium. Higher levels of occupancy by L are accompanied by a decrease in the amplitude of the peak centered on 10 nM A relative to the level of binding at lower concentrations of A (Figure 10B), in agreement with the patterns obtained with gallamine and *N*-[^{3}H]methylscopolamine (Figure 4). Similarly, the fitted values of K_j and F_j from Equation 3 ($n = 2$) vary with the concentration of L in a manner that resembles the corresponding changes observed experimentally (cf. Table S15 and Table 4).

BINDING OF ORTHOSTERIC ANTAGONISTS

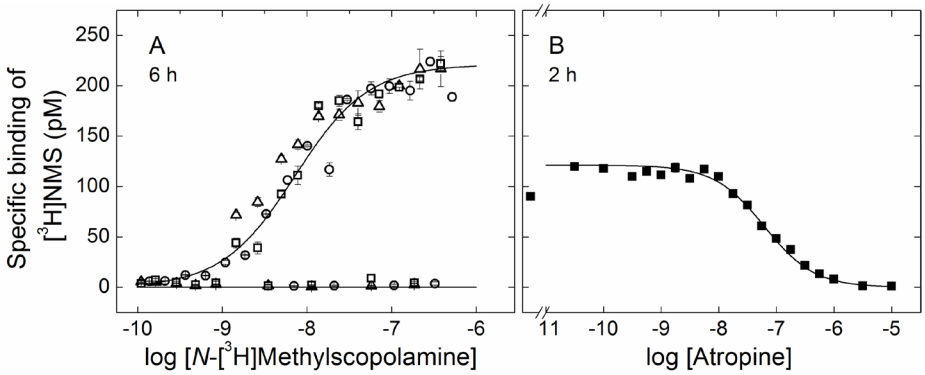

Figure S3. Binding of orthosteric antagonists to solubilized M_2 receptor from porcine atria. (A) Total binding of [^{3}H]NMS was measured after incubation of the receptor for 6 h at 30 °C with the radioligand alone (upper curves) or together with 1 mM unlabeled NMS (baseline). Different symbols denote data from different experiments (N = 3). (B) Total binding was measured after incubation of the receptor for 2 h at 30 °C with [^{3}H]NMS (10 nM) and atropine at the concentrations shown on the abscissa (N = 3). The lines depict the best fit of Scheme 1 to the data in both panels taken together. A single value of log K_P ([^{3}H]NMS) was common to all of the data, and a single value of log K_A (atropine) was common to the data represented in panel B. The fitted parametric values are as follows: log K_P = −8.15 ± 0.02, log K_A = −7.56 ± 0.01, $[R]_t$ = 226 ± 3.5 pM.

Table S1. Affinity of Orthosteric Antagonists for the M_2 Receptor in Various Preparations[a]

	log K		
tissue	QNB [b]	NMS [b]	atropine [c]
porcine sarcolemma			
membranes	−10.68 ± 0.04 (2)	−10.03 ± 0.03 (2)	−9.37 ± 0.01 (2)
CHL-depleted membranes	−10.77 ± 0.04 (2)	−10.03 ± 0.04 (2)	−9.41 ± 0.01 (2)
solubilised	−8.88 ± 0.02 (2)	−8.15 ± 0.02 (3)	−7.56 ± 0.01 (2)
*Sf*9 cells			
membranes	*d*	−9.31 ± 0.03 (2)	*d*
solubilised	−8.47 ± 0.01 (2)	−7.98 ± 0.04 (2)	−7.50 ± 0.06 (2)
CHO cells			
membranes	−10.66 ± 0.04 (9)	−10.01 ± 0.02 (3)	−9.44 ± 0.04 (3)

[a] Total binding was measured at graded concentrations of [^{3}H]QNB or [^{3}H]NMS (*e.g.*, Figure S3A) or at a constant concentration of [^{3}H]NMS (10 ± 0.1 nM) and graded concentrations of atropine (*e.g.*, Figure S3B). The data were analyzed in terms of Equation 2 or Scheme 1 to obtain the values of log K or log K_A, respectively, listed in the table. The number of independent experiments is shown in parentheses.
[b] Analyzed in terms of Equation 2 with the value of n_H fixed at 1.
[c] Analyzed in terms of Scheme 1. The value of K_P either was determined independently or was defined in the analysis by data at graded concentrations of [^{3}H]NMS.
[d] Not measured.

KINETICS OF DISSOCIATION

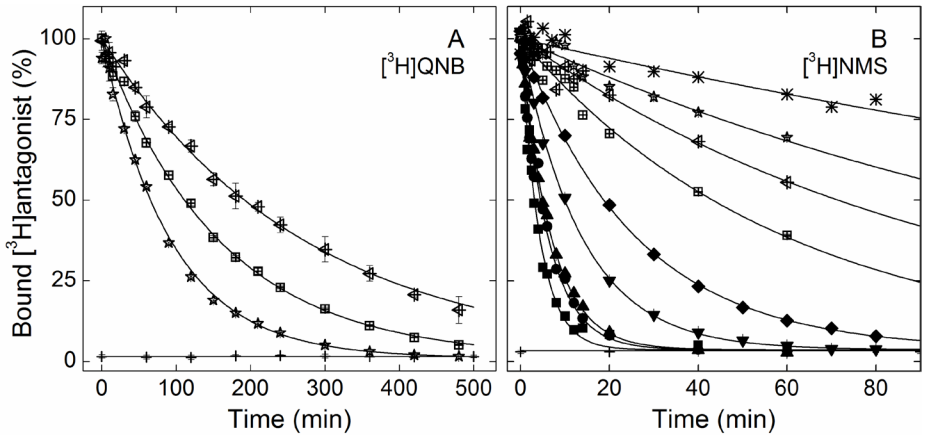

Figure S4. Effect of gallamine on the net dissociation of [^{3}H]quinuclidinylbenzilate (A) and *N*-[^{3}H]methylscopolamine (B) from solubilized M_2 receptor from porcine atria. Receptor was incubated with [^{3}H]QNB (1 nM) for 2 h or with [^{3}H]NMS (10 nM) for 45 min. Net dissociation of the radioligand was initiated by the addition of atropine at a final concentration of 3.0 μM, either alone (A, □; B, ■) or together with gallamine at the following concentrations (μM): panel A, 3.16 (✯), 31.6 (◁); panel B, 0.560 (●), 0.750 (▲), 3.20 (▼), 7.50 (♦) 10.0 (□), 32.0 (◁), 56 (✯), 100 (✳). Total binding then was measured at the times shown on the abscissa. Nonspecific binding was measured in a parallel assay in which the radioligand was accompanied by 3 μM atropine (+, baseline). The lines depict the best fit of Equation 1 to all data shown in the same panel. Separate values of $B_{t=0}$ and k_{obsd} were assigned to the data at each concentration of gallamine, and a single value of $B_{t\rightarrow\infty}$ was common to all of the data, including that obtained for nonspecific binding. The fitted values of the rate constants are as follows (min^{-1}): panel A, 0.0061 ± 0.0003 (□), 0.0109 ± 0.0005 (✯), and 0.0032 ± 0.0003 (◁); panel B, 0.219 ± 0.004 (■), 0.164 ± 0.006 (●), 0.147 ± 0.005 (▲), 0.074 ± 0.002 (▼), 0.039 ± 0.001 (◆) 0.017 ± 0.006 (□), 0.010 ± 0.006 (◁), 0.0072 ± 0.0004 (✯), and 0.0031 ± 0.0004 (✳)

MONOEXPONENTIAL NATURE OF THE NET DISSOCIATION OF AN ORTHOSTERIC LIGAND

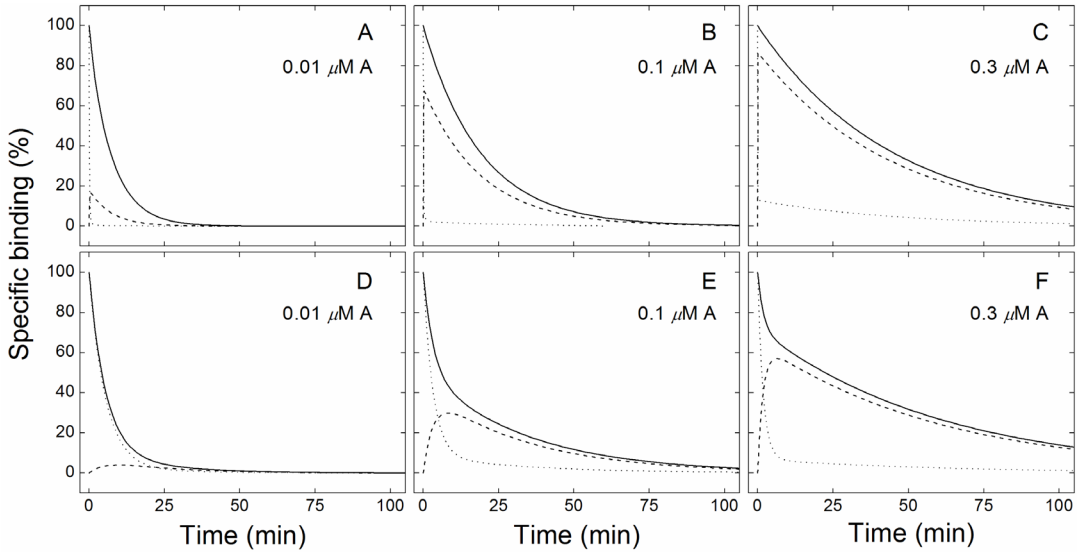

Figure S5. Net dissociation of a radiolabeled orthosteric ligand from a monomeric receptor in the presence of an unlabeled allosteric ligand. The data were simulated according to the scheme shown below in which R is the receptor, L is the orthosteric probe, and A is the allosteric ligand.

$$A+R+L \xleftarrow{k_{-1}} A+RL \underset{k_{-2}}{\overset{k_{+2}}{\rightleftharpoons}} ARL \xrightarrow{k_{-3}} AR+L$$

Net dissociation is initiated and maintained by an unlabeled orthosteric ligand (not shown), which is present at a saturating concentration and precludes binding of free radioligand. The allosteric ligand binds reversibly to RL with rate constants k_{+2} and k_{-2}, respectively. The radioligand dissociates from RL and ARL with rate constants k_{-1} and k_{-3}, respectively. The broken lines depict the simulated values of [RL] (• • •) and [ARL] (– – –). The solid lines depict the sum of those species occupied by L (*i.e.*, [RL] + [ARL]), as would be measured in a binding assay with a radioligand (*e.g.*, [^{3}H]NMS or [^{3}H]QNB). The parametric values used in the simulations and the fitted values from a biexponential are listed in Table S2.

Two scenarios are presented in which the allosteric ligand interacts comparatively rapidly with the receptor (A–C) or comparatively slowly (D–F). Three concentrations of A were considered, as follows: 0.01 μM (A, D), 0.1 μM (B, E), and 0.3 μM (C, F). Values of [R], [RL], [AR], and [ARL] were obtained by numerical integration of the four simultaneous differential equations that define the system, integrating by means of the ODE23s subroutine in MATLAB R2008a. In each case, the simulated data are superimposable with the best fit of a biexponential. The biexponential nature of the time-course becomes discernible when the slower component represents 5% or more of the signal. That occurs when the first-order rate constant for dissociation of the allosteric ligand (k_{-2}) is within threefold or less of that for dissociation of the orthosteric ligand (k_{-1}), and it is independent of the pseudo-first-order rate constant for association of the allosteric ligand (*i.e.*, k_{+2}[A]). Accordingly, net dissociation of an orthosteric ligand will be well described by a single exponential at any concentration of an allosteric ligand that dissociates rapidly from the receptor.

Table S2. Parametric Values for the Net Dissociation of an Orthosteric Ligand from a Monomeric Receptor in the Presence of an Allosteric Ligand[a]

	simulation							analysis		
Figure S5	[A] (μM)	k_{-1} (min^{-1})	k_{-2} (min^{-1})	k_{+2} ($\mu M^{-1}min^{-1}$)	k_{-3} (min^{-1})	k_{-2}/k_{+2} (μM)	k_{-2}/k_{-1}	k_1 (min^{-1})	k_2 (min^{-1})	F_2
A	0.01	0.17	5.4	120	0.0002	0.045	31.8	6.52	0.139	0.995
B	0.1	0.17	5.4	120	0.0002	0.045	31.8	17.5	0.053	0.995
C	0.3	0.17	5.4	120	0.0002	0.045	31.8	41.6	0.022	0.996
D	0.01	0.17	0.054	1.2	0.0002	0.045	0.318	0.190	0.049	0.122
E	0.1	0.17	0.054	1.2	0.0002	0.045	0.318	0.315	0.029	0.507
F	0.3	0.17	0.054	1.2	0.0002	0.045	0.318	0.568	0.016	0.721

[a] The parametric values listed in the table were used to simulate the data shown in the corresponding panels of Figure S5. The rate constants selected for dissociation of the orthosteric ligand are those measured for [^{3}H]NMS in preparations of solubilized M_2 receptor from porcine atria (Figure S4). The rate constants selected for dissociation and association of the allosteric ligand are those reported for gallamine and the M_2 receptor in membranes from CHO cells (*1*). The simulated data for total binding of the orthosteric ligand were analyzed in terms of the equation $Y_{obsd} = Y_{t=0}[(1 - F_2)e^{-k_1 t} + F_2 e^{-k_2 t}]$ to obtain the fitted values of k_1, k_2, and F_2 listed the table.

Table S3. Rate of Dissociation of [^{3}H]Quinuclidinylbenzilate from Membrane-bound M_2 Receptor[a]

preparation	[^{3}H]QNB (nM)	k_{obsd} (min^{-1})	$t_{1/2}$ (min)
Sf9 cells			
native membranes	0.20 (4)	0.020 ± 0.0004	35
membranes treated with DTT	0.20 (3)	0.057 ± 0.003	12
CHO cells (native membranes)			
	0.020 (8)	0.023 ± 0.006	32
	0.040 (4)	0.022 ± 0.003	32
	0.20 (9)	0.022 ± 0.002	37
	1.0 (9)	0.018 ± 0.005	41
	2.0 (4)	0.020 ± 0.004	35
	4.0 (3)	0.025 ± 0.002	28
porcine atria (native membranes)			
	0.020 (2)	0.014 ± 0.0001	50
	0.040 (1)	0.017 ± 0.0005	42
	0.20 (5)	0.016 ± 0.0009	44
	1.0 (1)	0.021 ± 0.0001	33
porcine atria (treated with methyl-β-cyclodextrin)			
	0.020 (2)	0.017 ± 0.0001	41
	0.040 (1)	0.015 ± 0.0001	46
	0.20 (2)	0.015 ± 0.0009	46
	1.0 (2)	0.014 ± 0.0001	47

[a] Membranes prepared from porcine atria, *Sf*9 cells, or CHO cells were incubated with [^{3}H]QNB for 60 min at 24 ºC. Net dissociation of the radioligand then was measured as described under 'Experimental Procedures' to obtain the rate constant, and values from different experiments were averaged to obtain the mean listed in the table. The number of independent experiments is shown in parentheses.

EFFECT OF IONIC COMPOSITION ON THE ALLOSTERIC EFFECT OF GALLAMINE

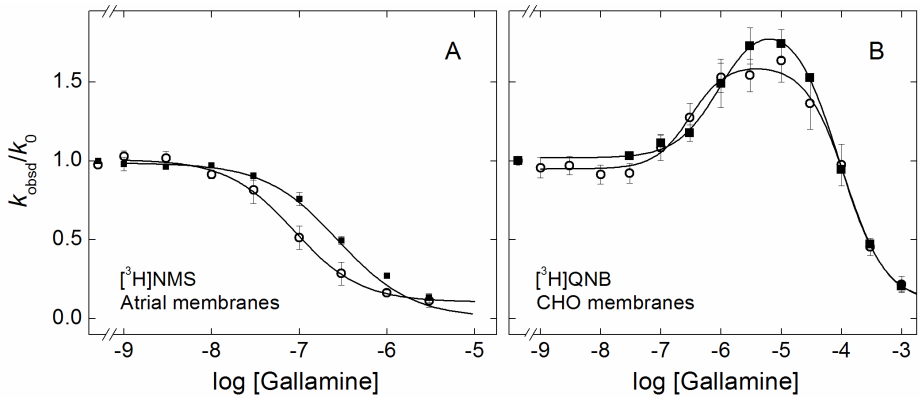

Figure S6. Effect of ionic composition and gallamine on the rate of dissociation of *N*-[^{3}H]methylscopolamine and [^{3}H]quinuclidinylbenzilate. Membranes from porcine atria (A) or CHO cells (B) were incubated with [^{3}H]NMS (1.0 nM, A) or [^{3}H]QNB (0.20 nM, B) in buffer B (■) or phosphate buffer (1 mM KH_2PO_4, 4 mM Na_2HPO_4, pH 7.4) (○). The concentration of Na^+ in buffer B was 31 mM. The normalized rate of dissociation (k_{obsd}/k_o) was measured at graded concentrations of gallamine, and values at the same concentration were averaged to obtain the means (± S.E.M.) plotted on the ordinate (N = 2–5). The lines depict the best fits of Equation 3, and the parametric values are listed in Table S4.

Table S4. Parametric Values for the Effect of Sodium and Gallamine on the Rate of Dissociation of *N*-[^{3}H]Methylscopolamine and [^{3}H]Quinuclidinylbenzilate[a]

radioligand	Na^+ (mM)	log K_1	log K_2	$n_{H(1)}$	$n_{H(2)}$	F_1	F_2	k_{obsd}/k_0 [G] = 0	k_{obsd}/k_0 [G]→∞
1.0 nM [^{3}H]NMS	4.0 (3)	−7.06 ± 0.09	—	1.14 ± 0.23	—	1.00	—	1.01 ± 0.03	0.10 ± 0.05
	20 (3)	−6.56 ± 0.07	—	1.04 ± 0.12	—	1.00	—	1.01 ± 0.01	0.07 ± 0.05
0.20 nM [^{3}H]QNB	4.0 (5)	−6.51 ± 0.18	−3.92 ± 0.08	1.48 ± 0.72	1.29 ± 0.44	−0.80	1.80[b]	0.95 ± 0.04	0.12 ± 0.14
	20 (2)	−6.02 ± 0.19	−4.05 ± 0.07	1.22 ± 0.34	1.15 ± 0.36	−1.00	2.00[b]	1.02 ± 0.05	0.10 ± 0.16

[a] The mean values of k_{obsd}/k_0 shown in Figure S6 were analyzed in terms of Equation 3 to obtain the parametric values listed in the table. The number of classes of sites (n) was taken as 1 for the effect of gallamine on the binding of [^{3}H]NMS to receptor in atrial membranes and 2 for the effect on the binding of [^{3}H]QNB to receptor in CHO membranes. The number of independent experiments is shown in parentheses.

[b] The value is defined by a shallow minimum in the sum of squares, as determined by mapping, and was fixed accordingly.

EFFECT OF DITHIOTHREITOL ON THE ALLOSTERIC EFFECT OF GALLAMINE

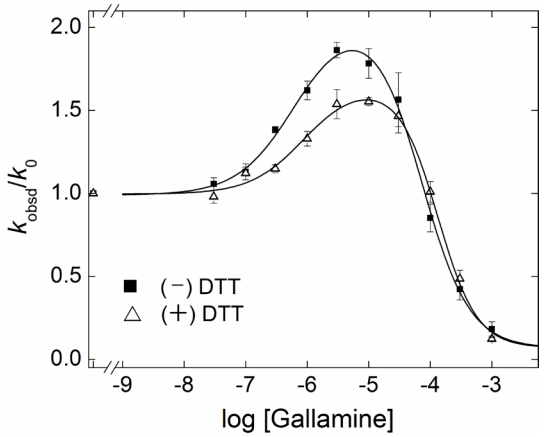

Figure S7. Effect of DTT and gallamine on the rate of dissociation of [^{3}H]quinuclidinylbenzilate from the M_2 receptor in *Sf*9 membranes. Membranes were incubated with [^{3}H]QNB (0.20 nM), and the normalized rate of dissociation (k_{obsd}/k_o) was measured at graded concentrations of gallamine in the absence (■) or presence (△) of DTT. Values at the same concentration of gallamine were averaged to obtain the means (± S.E.M.) plotted on the ordinate. The lines depict the best fits of Equation 3, and the parametric values are listed in Table S5.

Table S5. Parametric Values for the Effect of DTT and Gallamine on the Rate of Dissociation of [^{3}H]Quinuclidinylbenzilate from the M_2 Receptor in *Sf*9 Membranes[a]

DTT							k_{obsd}/k_0	
(mM)	log K_1	log K_2	$n_{H(1)}$	$n_{H(2)}$	F_1	F_2	[G] = 0	[G]→∞
0 (4)	−6.50 ± 0.09	−4.09 ± 0.05	1.18 ± 0.33	1.52 ± 0.25[b]	−1.10	2.10 ± 0.19	1.02 ± 0.04	0.07 ± 0.09
1 (3)	−6.05 ± 0.17	−3.88 ± 0.09	1.00 ± 0.52	1.37 ± 0.34	−0.72	1.72 ± 0.24	0.99 ± 0.03	0.17 ± 0.07

[a] The mean values of k_{obsd}/k_0 shown in Figure S7 were analyzed in terms of Equation 3 (n = 2) to obtain the parametric values listed in the table. The number of independent experiments is shown in parentheses.

[b] The value significantly exceeds 1 (P = 0.041).

EFFECT OF CHOLESTEROL ON THE ALLOSTERIC EFFECT OF GALLAMINE

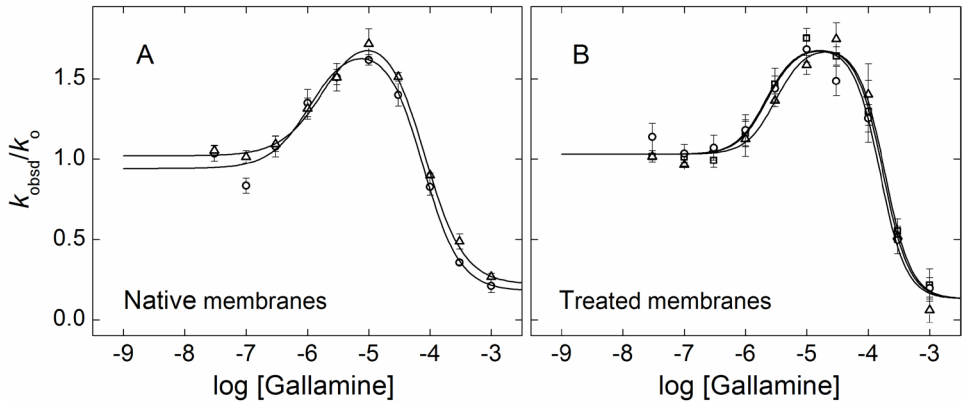

Figure S8. Effect of cholesterol, [^{3}H]quinuclidinylbenzilate, and gallamine on the rate of dissociation of [^{3}H]quinuclidinylbenzilate from the M_2 receptor in atrial membranes. Native membranes (A) or membranes pretreated with methyl-β-cyclodextrin (B) were incubated with [^{3}H]QNB (○, 0.02 nM; △, 0.20 nM; □, 1.0 nM), and the normalized rate of dissociation (k_{obsd}/k_o) was measured at graded concentrations of gallamine. Values at the same concentration of gallamine were averaged to obtain the means (± S.E.M.) plotted on the ordinate. The lines depict the best fit of Equation 3 (n = 2) to all data in the same panel taken together, and the parametric values are listed in Table S6.

Table S6. Parametric Values for the Effect of Gallamine, Cholesterol, and [^{3}H]Quinuclidinylbenzilate on the Rate of Dissociation of [^{3}H]Quinuclidinylbenzilate from the M_2 Receptor in Atrial Membranes[a]

[^{3}H]QNB							k_{obsd}/k_0	
(nM)	log K_1	log K_2	$n_{H(1)}$	$n_{H(2)}$	F_1	F_2	[G] = 0	[G]→∞
native membranes								
0.02 (2)	−5.94 ± 0.19	−4.10 ± 0.09	1.27 ± 0.37	1.35 ± 0.25	−0.99	1.99 ± 0.23	0.95 ± 0.04	0.15 ± 0.08
0.20 (5)	−5.82 ± 0.16	−4.07 ± 0.07			−0.98	1.98 ± 0.20	1.00 ± 0.03	0.23 ± 0.06
methyl-β-cyclodextrin-treated membranes								
0.02 (2)	−5.65 ± 0.19	−3.81 ± 0.08	1.83 ± 0.98	2.03 ± 0.47	−0.75	1.75 ± 0.17	1.03 ± 0.05	0.13 ± 0.10
0.20 (2)	−5.51 ± 0.19	−3.73 ± 0.09						
1.00 (2)	−5.67 ± 0.20	−3.76 ± 0.09						

[a] The mean values of k_{obsd}/k_0 shown in Figure S8 were analyzed in terms of Equation 3 (n = 2) to obtain the parametric values listed in the table. Data from the same preparation were analyzed in concert. In the case of native membranes, single values of $n_{H(j)}$ were common to data acquired at both concentrations of [^{3}H]QNB; in the case of membranes treated with methyl-β-cyclodextrin, single values of F_2, $n_{H(j)}$, and the asymptotic values of k_{obsd}/k_0 were common to all of the data. These constraints were without significant effect on the sum of squares ($P > 0.05$). The number of independent experiments is shown in parentheses.

EFFECT OF [^{3}H]QUINUCLIDINYLBENZILATE ON THE ALLOSTERIC EFFECT OF GALLAMINE

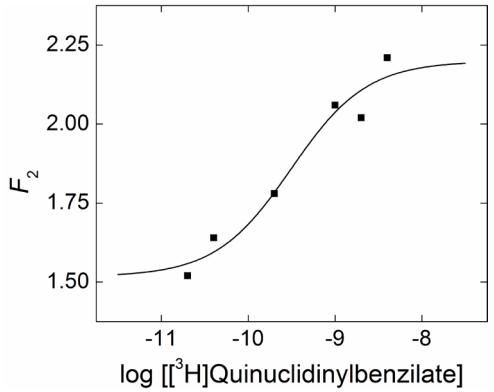

Figure S9. Effect of [^{3}H]quinuclidinylbenzilate on the amplitude of the peak in the bell-shaped dependence of k_{obsd}/k_0 on gallamine. M_2 receptor in CHO membranes was labeled at different concentrations of [^{3}H]QNB, and the rate of dissociation was measured at graded concentrations of gallamine (Figure 1D; Table 2). The data were analyzed in terms of Equation 3 to obtain the values of F_2 listed in Table 2 and plotted on the ordinate. The line depicts the best fit of Equation 3 (n = 1, $n_{H(1)}$ = 1), and the parametric values are as follows: K_1 = −9.51 ± 0.29, $Y_{[QNB]\to 0}$ = 1.52 ± 0.08, and $Y_{[QNB]\to \infty}$ = 2.20 ± 0.08.

LINEAR UNMIXING OF THE CONSTITUENT TERMS OF EQUATION 3

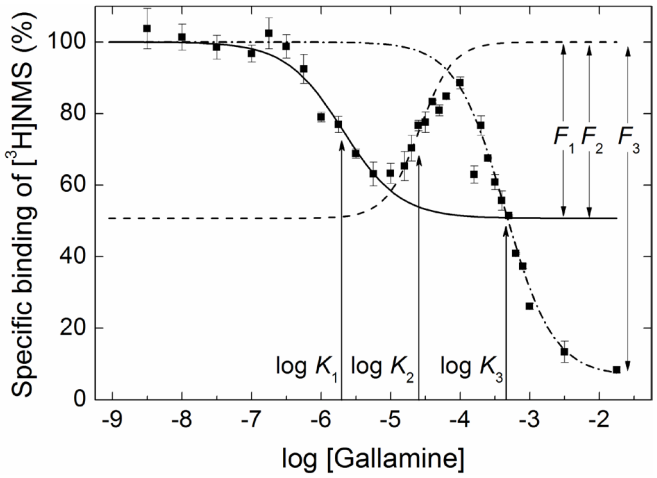

Figure S10. Empirical dissection of a triphasic, serpentine binding profile in terms of Equation 3. M_2 receptor was extracted from *Sf*9 cells, and binding was measured after incubation of the receptor with [^{3}H]NMS (10 nM) and gallamine for 21 h at 30 °C. The data have been replotted from Figure 3D, and the lines depict the constituent terms of Equation 3 (n = 3: j = 1, ——; j = 2, – – –; j = 3, – • –). The sum of those terms is the best fit of the model to the data, depicted by the line in Figure 3D, and the fitted parametric values are as follows: log K_1 = −5.69, −log K_2 = 4.59, −log K_3 = 3.36, $n_{H(1)}$ = 1.06, $n_{H(2)}$ = 1.82, $n_{H(3)}$ = 1.25, F_1 = 0.56, F_2 = −0.56, and F_3 = 1.00 (Table 3).

NATURE OF THE INSTABILITY IN ATRIAL EXTRACTS

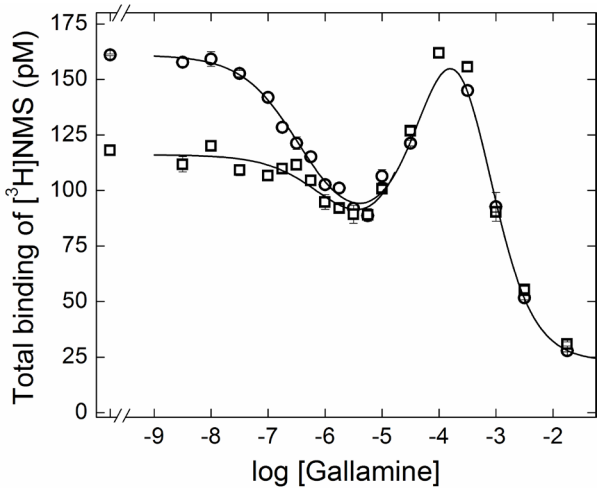

Figure S11. Instability of the M_2 receptor in atrial extracts. Aliquots of the extract were mixed simultaneously with [^{3}H]NMS (10 nM) and gallamine at the concentrations shown on the abscissa. Two sets of samples were prepared in parallel and incubated for 9 h (○) or 21 h (□) at 37 °C. The data are from one of two such experiments. The lines depict the best fit of Equation 3 (n = 3) to the pooled data from several experiments in which the samples were incubated for different times from 6 h to 30 h. The data from that analysis are shown in Figure 2, and the parametric values are listed in Table 3.

EFFECT OF GALLAMINE AT THE M_2 RECEPTOR IN MEMBRANES FROM *Sf*9 AND CHO CELLS

Table S7. Parametric Values for the Effect of *N*-[^{3}H]Methylscopolamine and Time of Incubation on the Binding of Gallamine to the M_2 Receptor in Mammalian Membranes[a]

[^{3}H]NMS (nM)	time	log K_1	log K_2	log K_3	$n_{H(1)}$	F_1	F_2	F_3
porcine atria								
0.10	3 h (4)	−7.27 ± 0.03	−3.44 ± 2.00	—	1.26 ± 0.11	0.97	0.03 ± 0.02	*b*
0.10	16 h (4)	−7.04 ± 0.04	−3.98 ± 1.45	−1.97 ± 2.03	1.52 ± 0.25[c]	0.94	−0.05[d]	0.11 ± 0.05
0.10	48 h (3)	−6.32 ± 0.05	−3.56 ± 2.19	−2.43 ± 3.41	3.48 ± 1.16[c]	1.00	−0.15 ± 0.57	0.15 ± 0.56
0.10	5 d (2)	−6.00 ± 0.07	−3.73 ± 1.26	−2.25 ± 1.73	3.95 ± 1.37[c]	1.01	−0.20[d]	0.19 ± 0.13
0.30	3 h (3)	−7.10 ± 0.03	−3.40 ± 0.53	—	1.34 ± 0.12	0.93	0.07 ± 0.02	*b*
0.30	48 h (3)	−5.89 ± 0.03	−4.33 ± 0.52	−2.08 ± 0.77	2.64 ± 0.36[c]	1.06	−0.25 ± 0.07	0.19 ± 0.06
0.30	5 d (3)	−5.69 ± 0.08	−4.01 ± 0.70	−2.08 ± 0.89	1.45 ± 0.31[c]	1.05	−0.28 ± 0.13	0.23 ± 0.06
1.0	3 h (3)	−6.75 ± 0.05	−3.04 ± 0.28	—	1.49 ± 0.16	0.82	0.18 ± 0.02	*b*
1.0	48 h (3)	−5.79 ± 0.03	−3.66 ± 0.45	−2.23 ± 0.40	3.14 ± 0.52[c]	0.90	−0.41 ± 0.18	0.51 ± 0.18
1.0	5 d (3)	−5.64 ± 0.03	−3.45 ± 0.36	−2.60 ± 0.26	4.61 ± 1.16[c]	0.86	−0.50[d]	0.64 ± 0.09
3.0	3 h (3)	−6.55 ± 0.05	−2.63 ± 0.17	—	1.14 ± 0.13	0.70	0.30 ± 0.03	*b*
3.0	48 h (3)	−5.73 ± 0.04	−3.89 ± 0.47	−2.57 ± 0.37	4.15 ± 1.00[c]	0.82	−0.55 ± 0.26	0.73 ± 0.29
3.0	5 d (3)	−5.53 ± 0.04	−4.32 ± 0.67	−2.36 ± 0.30	5.81 ± 2.97[c]	0.85	−0.56 ± 0.18	0.71 ± 0.15
CHO cells								
0.30	3 h (3)	−6.96 ± 0.02	−2.44 ± 1.13	—	1.11 ± 0.05	0.97	0.03 ± 0.04	*b*
0.30	16 h (3)	−6.16 ± 0.04	−4.38 ± 1.29	−1.98 ± 1.21	1.54 ± 0.19[c]	0.97	−0.09[d]	0.12 ± 0.07
0.30	48 h (3)	−5.93 ± 0.02	−3.65 ± 1.08	−2.77 ± 1.14	2.71 ± 0.39[c]	0.99	−0.24 ± 0.50	0.25 ± 0.50
1.0	3 h (3)	−6.72 ± 0.05	−3.14 ± 0.39	—	1.17 ± 0.11	0.90	0.10 ± 0.02	*b*
1.0	16 h (3)	−5.98 ± 0.02	−4.18 ± 0.42	−2.47 ± 0.40	2.45 ± 0.31[c]	0.96	−0.24 ± 0.06	0.28 ± 0.05
1.0	48 h (3)	−5.80 ± 0.02	−3.71 ± 0.50	−2.82 ± 0.69	3.14 ± 0.31[c]	1.01	−0.53 ± 0.62	0.52 ± 0.60
3.0	3 h (3)	−6.44 ± 0.04	−2.84 ± 0.41	—	1.27 ± 0.11[c]	0.75	0.25 ± 0.02	*b*
3.0	16 h (3)	−5.79 ± 0.04	−4.31 ± 0.41	−2.55 ± 0.38	2.41 ± 0.38[c]	0.94	−0.54 ± 0.11	0.58 ± 0.12
3.0	48 h (3)	−5.71 ± 0.06	−4.37 ± 0.54	−2.91 ± 0.39	2.20 ± 0.39[c]	1.08	−0.75 ± 0.22	0.63 ± 0.28

[a] The data represented in Figure 5 were analyzed in terms of Equation 3 (n = 1 or 2) to obtain the parametric values listed in the table. Data acquired under different conditions were analyzed separately. Data from experiments performed under the same conditions were analyzed in concert, with single values of log K_j, $n_{H(1)}$, and F_j common to all sets within the analysis. All values of $n_{H(2)}$ and values of $n_{H(3)}$ at times greater than 3 h were not well defined and were fixed at 1; the constraint was without appreciable effect on the sum of squares ($P > 0.05$). The fitted values of $n_{H(3)}$ at each concentration of [^{3}H]NMS after 3 h are as follows: porcine atria, 0.1 nM, 1.00; 0.3 nM, 1.14 ± 1.21; 1.0 nM, 1.36 ± 0.81; 3.0 nM, 0.64 ± 0.27; CHO cells, 0.3 nM, 1.04 ± 2.10; 1.0 nM, 1.00 ± 0.31; 3.0 nM, 0.82 ± 0.36. The number of independent experiments is shown in parentheses.

[b] Two classes of sites are sufficient to describe the data (n = 2).

[c] The value significantly exceeds 1 ($P < 0.05$).

[d] The value is defined by a shallow minimum in the sum of squares, as determined by mapping, and was fixed accordingly.

EFFECT OF *N*-[^{3}H]METHYLSCOPOLAMINE ON THE APPARENT AFFINITY OF GALLAMINE

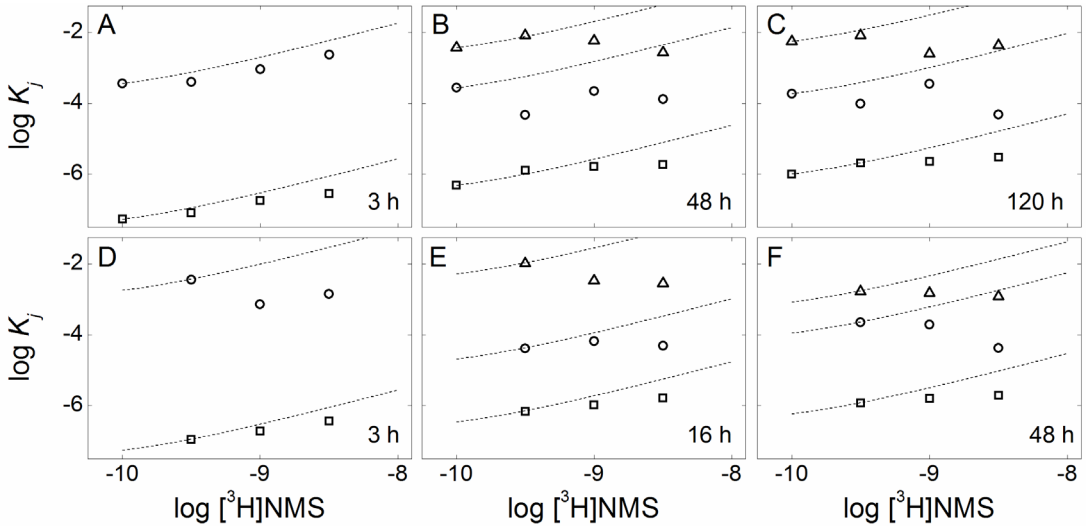

Figure S12. Apparent affinity of gallamine at different concentrations of *N*-[^{3}H]methylscopolamine. Membranes from porcine atria (A–C) or CHO cells (D–F) were mixed simultaneously with [^{3}H]NMS and gallamine at graded concentrations of the latter, and total binding was measured after incubation of the samples at 24 ºC for the time shown in each panel. The concentration of [^{3}H]NMS is plotted on the abscissa (*i.e.*, 0.1 nM, 0.3 nM, 1.0 nM, or 3.0 nM). Data from several experiments were pooled and analyzed in terms of Equation 3 (n = 3), and the fitted values of log K_1 (□), log K_2 (○), and log K_3 (△) obtained for gallamine are plotted on the ordinate. The data are shown in Figure 5, and the parametric values are listed in Table S7. The dotted lines show the expected dependence of log K_j on the concentration of [^{3}H]NMS if the interaction were competitive. The value of K_j at each concentration of [^{3}H]NMS was calculated according to the equation $K_j = K_A(1+[P]/K_P)$, where K_A and K_P are the equilibrium dissociation constants of gallamine and [^{3}H]NMS, respectively, and [P] is the concentration of [^{3}H]NMS. The values of K_P are listed in Table S1. A value of K_A was calculated for each K_j in each panel according to the equation $K_A = K_{j,low}/(1+[P]/K_P)$, where $K_{j,low}$ is K_j at the lowest concentration of [^{3}H]NMS (*i.e.*, 0.1 nM and 0.3 nM for membranes from porcine atria and CHO cells, respectively).

EFFECT OF DEPLETED CHOLESTEROL ON THE INTERACTION BETWEEN GALLAMINE AND *N*-[^{3}H]METHYLSCOPOLAMINE

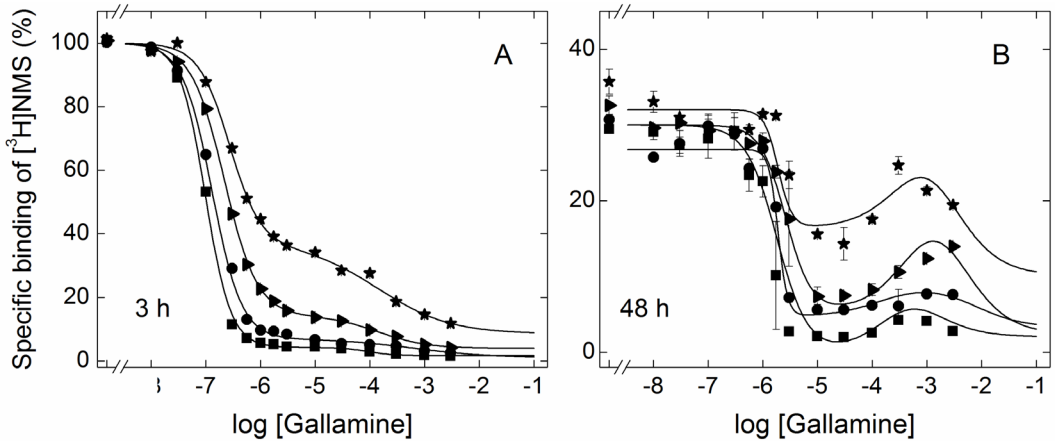

Figure S13. Effect of *N*-[^{3}H]methylscopolamine and time of incubation on the allosteric effect of gallamine at the M_2 receptor in cholesterol-depleted membranes. Atrial membranes were depleted of cholesterol by means of methyl-β-cyclodextrin and mixed simultaneously with [^{3}H]NMS (0.1–3.0 nM) and gallamine at the concentrations shown on the abscissa. The concentrations of [^{3}H]NMS were as follows: 0.1 nM (■), 0.3 nM (●), 1.0 nM (▶), and 3.0 nM (★). Total binding was measured after incubation of the mixture for 3 h (A) or 48 h (B) at 24 °C. The lines represent the best fits of Equation 3 (n = 2 or 3) to data acquired at the same time and concentration of [^{3}H]NMS, and the parametric values are listed in Table S9.

Table S8. Parametric Values for the Effect of *N*-[^{3}H]Methylscopolamine and Time of Incubation on the Allosteric effect of Gallamine at the M_2 Receptor in Cholesterol-depleted Membranes[a]

[^{3}H]NMS (nM)	time (h)	log K_1	log K_2	log K_3	$n_{H(1)}$	F_1	F_2	F_3
0.10	3 (1)	−7.02 ± 0.04	−3.94 ± 1.31	—	1.87 ± 0.23	0.97	0.03 ± 0.02	*b*
0.10	48 (2)	−5.75 ± 0.13	−3.48 ± 8.56	−3.17 ± 11.3	1.53 ± 0.48	1.07	−1.00 ± 6.00	0.93 ± 6.0
0.30	3 (1)	−6.86 ± 0.01	−3.43 ± 0.53	—	1.60 ± 0.10	0.95	0.05 ± 0.02	*b*
0.30	48 (2)	−5.72 ± 0.02	−3.82 ± 1.31	−2.13 ± 1.18	5.06 ± 1.70	0.94	−0.19 ± 0.18	0.25 ± 0.19
1.0	3 (1)	−6.66 ± 0.01	−3.89 ± 0.16	—	1.49 ± 0.16	0.90	0.10 ± 0.00	*b*
1.0	48 (2)	−5.58 ± 0.07	−3.05 ± 0.20	−2.60[c]	1.86 ± 0.34	0.90	−1.49 ± 0.63	1.60 ± 0.67
3.0	3 (1)	−6.55 ± 0.02	−3.78 ± 0.01	—	1.46 ± 0.07	0.74	0.26 ± 0.01	*b*
3.0	48 (2)	−5.72[b]	−3.12 ± 1.74	−2.74 ± 1.65	3.42 ± 1.55	0.71	−1.56 ± 12.3	1.85 ± 12.3

[a] The data represented in Figure S13 were analyzed in terms of Equation 3 (n = 2 or 3) to obtain the parametric values listed in the table. The values of $n_{H(2)}$ and $n_{H(3)}$ were not well defined and were fixed at 1 without a significant increase in the sum of squares (P > 0.05). The number of independent experiments is shown in parentheses.

[b] Two classes of sites are sufficient to describe the data (n = 2).

[c] The value is defined by a shallow minimum in the sum of squares, as determined by mapping, and was fixed accordingly.

EFFECT OF IONIC STRENGTH ON THE INTERACTION BETWEEN GALLAMINE AND *N*-[^{3}H]METHYLSCOPOLAMINE

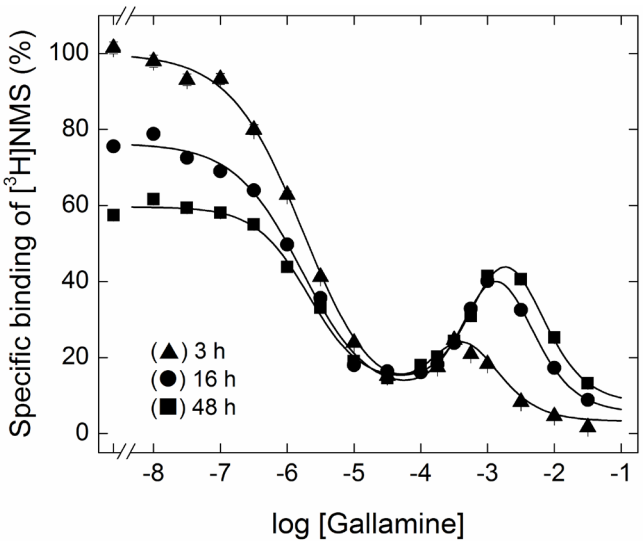

Figure S14. Allosteric effect of gallamine on the binding of *N*-[^{3}H]methylscopolamine to the M_2 receptor after incubation for different times at high ionic strength. Membranes from CHO cells were mixed simultaneously with gallamine and [^{3}H]NMS (1 nM) in Dulbecco's phosphate-buffered saline (1.47 mM KH_2PO_4, 8.10 mM Na_2HPO_4, 2.68 mM KCl, 137 mM NaCl, pH 7.4) (Sigma-Aldrich) supplemented with $CaCl_2$ (1 mM) and $MgCl_2$ (1 mM). Total binding was measured after incubation of the reaction mixture for 3 h (▲), 16 h (●), and 48 h (■) at 24 °C. The lines depict the best fit of Equation 3, and the parametric values are listed in Table S9.

Table S9. Parametric Values for the Allosteric Effect of Gallamine on the Binding of *N*-[^{3}H]Methylscopolamine at High Ionic Strength [a]

time (h)	log K_1	log K_2	log K_3	$n_{H(1)}$	$n_{H(2)}$	$n_{H(3)}$	F_1	F_2	F_3
3 (1)	−5.76 ± 0.09	−3.65 ± 0.34	−3.12 ± 0.63	0.79 ± 0.09			0.97	−0.49 ± 0.79	0.52 ± 0.82
16 (1)	−5.78 ± 0.08	−3.20 ± 0.09	−2.56 ± 0.10	0.86 ± 0.11	1.38 ± 0.22	1.21 ± 0.28	0.95	−1.00 [b]	1.05 ± 0.07
48 (1)	−5.68 ± 0.07	−3.10 ± 0.18	−2.36 ± 0.28	1.10 ± 0.16			0.90	−1.24 ± 0.74	1.34 ± 0.74

[a] The data represented in Figure S14 were analyzed in terms of Equation 3 (n = 3) to obtain the parametric values listed in the table. There was no appreciable increase in the sum of squares with single rather than separate values of $n_{H(2)}$ and $n_{H(3)}$ for data acquired after different times of incubation (P = 0.9).
[b] The value is defined by a shallow minimum in the sum of squares, as determined by mapping, and was fixed accordingly.

EFFECT OF SEQUENTIAL MIXING ON THE EQUILIBRATION OF GALLAMINE

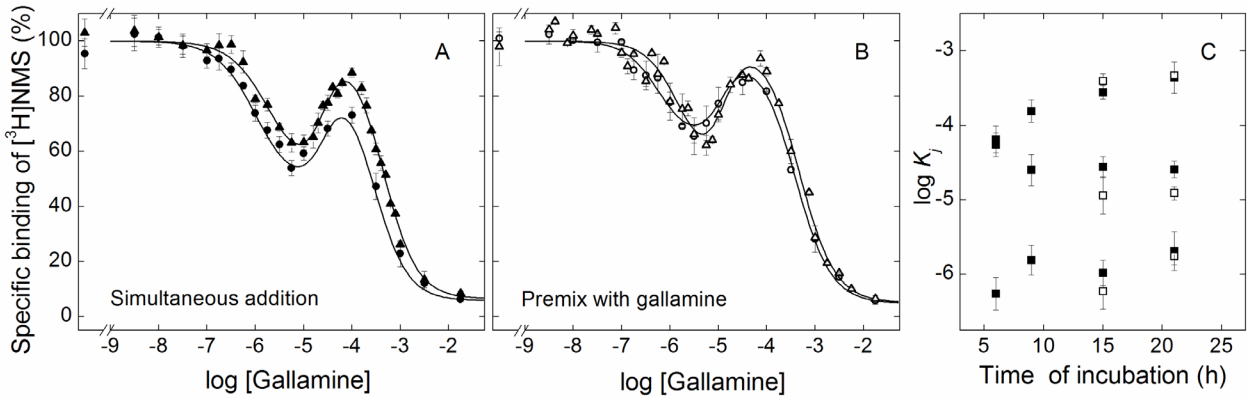

Figure S15. Effect of the order of mixing on the equilibration of gallamine and *N*-[^{3}H]methylscopolamine with solubilized M_2 receptor from *Sf*9 cells. Aliquots of the extract were mixed simultaneously with gallamine and [^{3}H]NMS (A, closed symbols) or first with gallamine and subsequently with [^{3}H]NMS after an interval of 2 h at 30 ºC (B, open symbols). Total binding was measured after further incubation of the samples for 15 h (○, ●) or 21 h (△, ▲) at 30 ºC. The lines depict the best fits of Equation 3 (n = 3) to all data represented in the same panel taken together, and the parametric values are listed in Table S10. The values of log K_j are compared in panel C (■, simultaneous addition; □, prior addition of gallamine), where those corresponding to incubation for 3 h and 9 h are from Table 3.

Table S10. Parametric Values for the Effect of the Order of Mixing on Equilibration of the Receptor with Gallamine and *N*-[^{3}H]Methylscopolamine[a]

time (h)	log K_1	log K_2	log K_3	$n_{H(1)}$	$n_{H(2)}$	$n_{H(3)}$	F_1	F_2	F_3
simultaneous mixing with gallamine and [^{3}H]NMS									
15 (5)	−5.98 ± 0.17	−4.56 ± 0.14	−3.56 ± 0.09	1.06 ± 0.21	1.82[b] ± 0.49	1.25 ± 0.09	0.58	−0.49 ± 0.15	0.91 ± 0.13
21 (4)	−5.69 ± 0.26	−4.59 ± 0.11	−3.36 ± 0.21				0.56	−1.00 ± 60.0	1.00[c]
premixing with gallamine									
15 (2)	−6.23 ± 0.01	−4.94 ± 0.25	−3.41 ± 0.10	1.25 ± 0.34	1.81[b] ± 0.51	1.18 ± 0.12	0.39	−0.35 ± 0.12	0.96 ± 0.08
21 (3)	−5.76 ± 0.02	−4.91 ± 0.09	−3.33 ± 0.05				0.56	−0.56[c]	1.00[c]

[a] The data represented in Figure S15 were analyzed in terms of Equation 3 (n = 3) to obtain the parametric values listed in the table. There was no appreciable effect on the sum of squares with single rather than separate values of $n_{H(j)}$ for data acquired after equilibration for 15 h and 21 h ($P > 0.05$). The number of independent experiments is shown in parentheses.

[b] The value significantly exceeds 1 ($P < 0.05$).

[c] The value is defined by a shallow minimum in the sum of squares, as determined by mapping, and was fixed accordingly.

Table S11. Parametric Values for the Effect of the Order of Mixing on the Equilibration of Gallamine and *N*-[^{3}H]Methylscopolamine with the M_2 Receptor in Membranes from Porcine Atria and *Sf*9 Cells[a]

time	log K_1	log K_2	log K_3	$n_{H(1)}$	$n_{H(2)}$	F_1	F_2	F_3
membranes from porcine atria after the simultaneous addition of gallamine and [^{3}H]HMS								
3 h (4)	−7.27 ± 0.03	−3.44 ± 2.00	—	1.26 ± 0.11	1[c]	0.97	0.03 ± 0.02	*f*
16 h (4)	−7.04 ± 0.04	−3.98 ± 1.45	−1.97 ± 2.03	1.52 ± 0.25[b]	1[c]	0.94	−0.05[e]	0.11 ± 0.05
48 h (3)	−6.32 ± 0.05	−3.56 ± 2.19	−2.43 ± 3.41	3.48 ± 1.16[b]	1[c]	1.00	−0.15 ± 0.57	0.15 ± 0.56
5 d (2)	−6.00 ± 0.07	−3.73 ± 1.26	−2.25 ± 1.73	3.95 ± 1.37[b]	1[c]	1.01	−0.20[e]	0.19 ± 0.13
membranes from *Sf*9 cells after the simultaneous addition of gallamine and [^{3}H]NMS								
3 h (3)	−7.13 ± 0.06	−4.56 ± 0.03	−4.53 ± 0.22	1.26 ± 0.17	1.82[d]	0.73	−0.30 ± 0.22	0.57 ± 0.24
16 h (5)	−6.77 ± 0.06	−4.33 ± 0.14	−3.72 ± 0.42	0.86 ± 0.08		0.90	−0.42 ± 0.34	0.52 ± 0.34
48 h (4)	−6.12 ± 0.09	−3.82 ± 0.04	−3.13 ± 0.07	4.64 ± 2.97		0.89	−0.74 ± 0.05	0.85[d]
5 d (2)	−5.97 ± 0.05	−3.81 ± 0.10	−2.64 ± 0.27	3.44 ± 1.00		0.84	−0.72 ± 0.18	0.88 ± 0.18
membranes from porcine atria after premixing with [^{3}H]NMS								
3 h (3)	−6.86 ± 0.01	−3.43 ± 0.53		1.60 ± 0.10	0.73 ± 0.21		*g*	*f*
16 h (3)	−5.72 ± 0.02	−3.82 ± 1.31		5.06 ± 1.70	1.29 ± 1.46		*g*	*f*
48 h (1)	−6.86 ± 0.01	−3.43 ± 0.53		1.60 ± 0.10	1.78 ± 1.53		*g*	*f*
5 d (1)	−5.72 ± 0.02	−3.82 ± 1.31		5.06 ± 1.70	1.35 ± 2.73		*g*	*f*
membranes from *Sf*9 cells after premixing with [^{3}H]NMS								
3 h (3)	−7.19 ± 0.06	−3.95 ± 0.04		1.04 ± 0.13	1.50 ± 0.20[b]		*g*	*f*
16 h (5)	−6.54 ± 0.05	−3.66 ± 0.06		1.51 ± 0.17			*g*	*f*
48 h (2)	−6.08 ± 1.44	−3.34 ± 0.09		7.25 ± 11.6			*g*	*f*
5 d (2)	−5.97 ± 2.61	−3.62 ± 0.29		7.33 ± 27.6			*g*	*f*

[a] The data represented in Figure 7 were analyzed in terms of Equation 3 (n = 2 or 3) to obtain the parametric values listed in the table. The concentration of [^{3}H]NMS was 0.3 nM throughout. Data obtained from the same preparation and after the same order of mixing were analyzed in concert; those obtained after different periods of incubation shared a single value of $n_{H(2)}$ where indicated by the brackets. The values of $n_{H(3)}$ following simultaneous addition of the ligands were not well defined and were fixed at the corresponding values for the solubilized receptor from porcine atria (1.00) and *Sf*9 cells (1.25) (Table 3). Such constraints on $n_{H(j)}$ were without appreciable effect on the sum of squares ($P > 0.05$). The number of independent experiments is shown in parentheses.

[b] The value significantly exceeds 1 ($P < 0.05$).

[c] The value is not well defined and was fixed at 1.

[d] The value is not well defined and was fixed at that obtained for the solubilized receptor (Table 3).

[e] The value is defined by a shallow minimum in the sum of squares, as determined by mapping, and was fixed accordingly.

[f] Two classes of sites (n = 2).

[g] Owing to the small difference in value between $Y_{[G]\rightarrow 0}$ and $Y_{[G]\rightarrow \infty}$, the value of F_2 is not defined.

KINETIC DESCRIPTION OF THE INTERACTION BETWEEN GALLAMINE AND *N*-[^{3}H]METHYLSCOPOLAMINE WITHIN A MONOMERIC RECEPTOR

Table S12. Rate constants for the Simulated Binding of Gallamine and *N*-[^{3}H]Methylscopolamine According to Scheme 2[a]

equilibrium dissociation constant			rate constants		
	value			value	
Parameter	$\alpha = 1$	$\alpha = 46$	parameter	$\alpha = 1$	$\alpha = 46$
K_L	1.00×10^{-8} M	1.00×10^{-8} M	k_{-L} k_{+L}	0.20 min^{-1} 2.0×10^7 M^{-1} min^{-1}	0.20 min^{-1} 2.0×10^7 M^{-1} min^{-1}
K_{LA}	1.00×10^{-8} M	4.60×10^{-7} M	k_{-LA} k_{+LA}	0.20 min^{-1} 2.0×10^7 M^{-1} min^{-1}	4.4×10^{-3} min^{-1} 9.5×10^3 M^{-1} min^{-1}
K_A	4.07×10^{-9} M	4.07×10^{-9} M	k_{-A} k_{+A}	1.3 min^{-1} 3.2×10^8 M^{-1} min^{-1}	1.3 min^{-1} 3.2×10^8 M^{-1} min^{-1}
K_{AL}	4.07×10^{-9} M	1.87×10^{-7} M	k_{-AL} k_{+AL}	1.3 min^{-1} 3.2×10^8 M^{-1} min^{-1}	1.3 min^{-1} 6.9×10^6 M^{-1} min^{-1}

[a] The rate constant for the association of [^{3}H]NMS with a vacant receptor (k_{+L}) was calculated according to Equation S1 from the equilibrium dissociation constant ($K_L = 1 \times 10^{-8}$ M, Table S1) and the rate constant of dissociation ($k_{-L} = 0.2$ min^{-1}, Figure S4). The rate constant for the association of gallamine with a vacant receptor (k_{+A}) was calculated according to Equation S2 from the equilibrium dissociation constant and the rate constant of dissociation reported previously [$K_A = 4.07 \times 10^{-9}$ M (*8*), $k_{-A} = 1.3$ min^{-1} (*8*)]. The rate constants for the binding of either ligand in the presence of the other were calculated according to Equations S7–S10; the value of α was taken as 1 or 46 (*9*), and the rate of dissociation of the allosteric ligand was taken as the same with or without the orthosteric ligand (*i.e.*, $k_{-AL} = k_{-A}$) (*8*). The values of k listed in the table were used to compute the curves presented in Figure S16.

KINETIC DESCRIPTION OF THE INTERACTION BETWEEN GALLAMINE AND *N*-[^{3}H]METHYL-SCOPOLAMINE WITHIN A MONOMERIC RECEPTOR

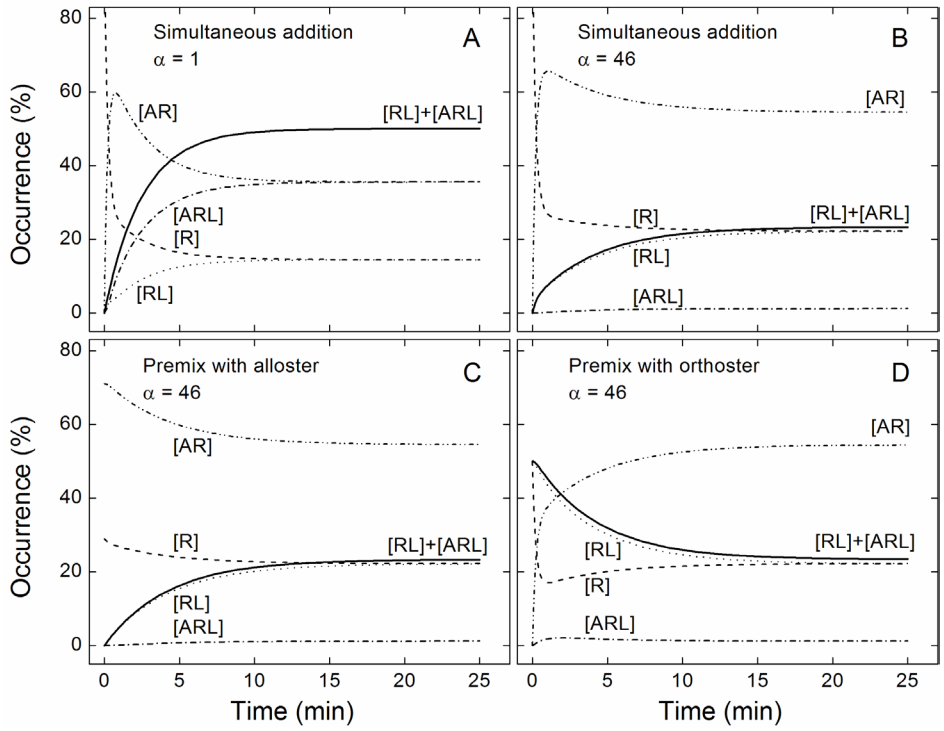

Figure S16. Time-dependent binding of gallamine and *N*-[^{3}H]methylscopolamine to a monomeric receptor. The data were simulated according to Scheme 2, where the allosteric (A) and orthosteric (L) ligands represent gallamine and [^{3}H]NMS, respectively. Further details regarding the simulations are described in the text accompanying Scheme 2 (page S-2). The broken lines depict the time-course for the appearance or loss of each species of receptor in the model (– – –, [R]; •••, [RL]; – ••–, [AR]; – • – •–, [ARL]). The solid lines depict the time-course for the sum of those species occupied by the orthosteric ligand (*i.e.*, [RL] + [ARL]), as would be measured in a binding assay with a radioligand such as [^{3}H]NMS. All parametric values are listed in Table S12 for $\alpha = 1$ (panel A) and $\alpha = 46$ (panels B–D) (*9*). The total concentration of receptor is 100 units throughout, and the free concentration of each ligand is 10 nM. The concentration of the orthosteric ligand therefore equals its equilibrium dissociation constant, as with [^{3}H]NMS in the present investigation. Initial time in the simulations corresponds experimentally to the earliest time at which both ligands are present with the receptor. The initial conditions therefore are as follows: (A and B) $[R]_0 = 100$ (simultaneous addition of A and L to the receptor); (C) $[R]_0 = 29$, $[AR]_0 = 71$ (premixing of the receptor with A); and (D) $[R]_0 = 50$, $[RL]_0 = 50$ (premixing of the receptor with L). In each panel, the trace for total bound orthosteric ligand is well described by a single exponential, and the fitted values of k_{obsd} are as follows (min^{-1}): 0.399 (A), 0.238 (B), 0.238 (C), and 0.239 (D).

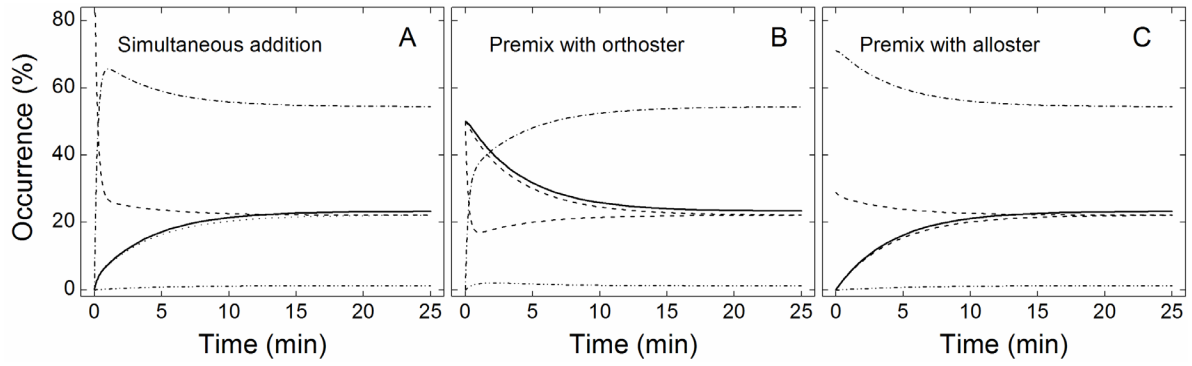

Figure S17. Time-dependent binding of gallamine and *N*-[^{3}H]methylscopolamine to a monomeric receptor. The data were simulated according to Scheme S1, where and the allosteric (A) and orthosteric (L) ligands represent gallamine and [^{3}H]NMS, respectively. Further details are described in the text accompanying Scheme S1 (page S-4). The broken lines depict the time-course for the appearance or loss of each species of receptor in the model (•••, [R]; – – –, [RL]; –••–, [AR]; –•–•–, [ARL]). The solid lines depict the time-course for the sum of those species occupied by the orthosteric ligand (*i.e.*, [RL] + [ARL]). All parametric values are listed in Table S12 (α = 46). The total concentration of receptor is 100 units, and the free concentration of each ligand is 10 nM. The initial conditions therefore are as follows: (A) $[R]_0$ = 100 (simultaneous addition of A and L to the receptor); (B) $[R]_0$ = 50, $[RL]_0$ = 50 (premixing of the receptor with L); and (C) $[R]_0$ = 29, $[AR]_0$ = 71 (premixing of the receptor with A). In each panel, the trace for total bound orthosteric ligand is well described by a single exponential, and the fitted values of k_{obsd} are as follows (min^{-1}): 0.300 (A), 0.226 (B), and 0.239 (C).

Table S13. Apparent Rate Constants for the Equilibration of Gallamine and *N*-[^{3}H]Methylscopolamine with a Monomeric Receptor[a]

	initial conditions					
	simultaneous mixing		premix with orthoster (L)		premix with alloster (A)	
log [A]	k_{obsd} (min^{-1})	$t_{½}$ (min)	k_{obsd} (min^{-1})	$t_{½}$ (min)	k_{obsd} (min^{-1})	$t_{½}$ (min)
−8.0	0.300	2.31	0.226	3.07	0.239	2.90
−7.5	0.234	2.96	0.191	3.63	0.188	3.69
−7.0	0.151	4.59	0.142	4.87	0.133	5.21
−6.5	0.0787	8.81	0.0822	8.43	0.0742	9.34
−6.0	0.0331	20.9	0.0355	19.5	0.0317	21.9
−5.0	0.00420	165	0.00510	136	0.00380	182
−4.0	0.000700	990	0.00150	462	0.000400	1,733

[a] The time-course for the appearance or loss of each species of receptor in Scheme S1 was simulated with the parametric values listed in Table S12 (α = 46) for the initial conditions shown in the table. Gallamine and [^{3}H]NMS correspond to the allosteric (A) and orthosteric (L) ligands, respectively. Simulations were performed at the free concentrations of A listed in the table; the free concentration of L was 10 nM throughout, and the total concentration of receptor was 100 units. At each concentration of A, the trace for total bound orthosteric ligand (*i.e.*, [RL] + [ARL]) is well described by a single exponential; the fitted values of k_{obsd} and the corresponding values of $t_{½}$ are listed in the table. The data obtained when [A] = 10 nM are illustrated in Figure S17. Further details are described in Table S12 and the legend to Figure S16.

KINETIC DESCRIPTION OF THE INTERACTION BETWEEN GALLAMINE AND *N*-[^{3}H]METHYL-SCOPOLAMINE WITHIN A DIMERIC RECEPTOR

Table S14. Parametric Values for the Binding of Allosteric and Orthosteric Ligands to a Dimeric Receptor[a]

binding of L			binding of A		
product	log K[b]	α	product	log K[b]	α
R_{LO}^{OO}, R_{OL}^{OO}	−6.0	—	R_{OO}^{AO}, R_{OO}^{OA}	−8.0	—
R_{LL}^{OO}	−4.0	α_{LL}^{OO}, 100.0	R_{OO}^{AA}	−8.0	α_{OO}^{AA}, 1.000
R_{OL}^{AO}, R_{LO}^{OA}	−8.5	α_{OL}^{AO}, 0.0032	R_{OL}^{AO}, R_{LO}^{OA}	−10.5	α_{OL}^{AO}, 0.0032
R_{LO}^{AO}, R_{OL}^{OA}	−3.0	α_{LO}^{AO}, 1000	R_{LO}^{AO}, R_{OL}^{OA}	−5.0	α_{LO}^{AO}, 1000

[a] The data illustrated in Figure 10 were simulated according to the simultaneous differential equations that describe Scheme 3. The values of the rate constants for binding to a vacant dimer were as follows: k_{-A} = 1.3 min^{-1} (*8*), $k_{+A} = 1.3 \times 10^8$ M^{-1}min^{-1}, k_{-L} = 0.2 min^{-1} (cf. Figure S4), $k_{+L} = 2.0 \times 10^5$ M^{-1}min^{-1}. The values of the remaining 60 first- and second-order rate constants were calculated from the equilibrium dissociation constants and cooperativity factors listed in the table. Further details are described in the legend to Figure S2 and the accompanying text (pp. S-4–S-8).
[b] Microscopic dissociation constant.

Table S15. Empirical Description of the Allosteric Effects Predicted by Scheme 3[a]

	simulation (Scheme 3)								
		orthosteric ligand (L)		analysis (Equation 3)					
	time[b]	occupancy[c]	conc.						
curve	(min)	(%)	(nM)	log K_1	log K_2	$n_{H(1)}$	$n_{H(2)}$	F_1	F_2
Figure 10A									
a	5	38.7	316	−10.35	−7.85	1.00	1.01	−0.50	1.50
b	15	38.7	316	−10.19	−7.61	1.00	1.05	−1.12	2.12
c	equil.	38.7	316	−10.09	−5.77	1.00	1.00	−2.71	3.71
Figure 10B									
a	equil.	38.7	316	−10.09	−5.77	1.00	1.00	−2.71	3.71
b	equil.	52.9	562	−10.23	−5.57	1.00	1.00	−1.72	2.72
c	equil.	66.7	1,000	−10.32	−5.41	1.00	1.00	−1.15	2.15

[a] The simulated data in Figure 10 were analyzed in terms of Equation 3 (n = 2) to obtain the parametric values listed in the table.
[b] The level of binding was computed after 5 min, 15 min, and sufficient time for the system to attain equilibrium (equil.).
[c] The level of occupancy at those sites with a macroscopic dissociation constant of 10^{-6}/2 M (Table S14).

PRE-EQUILIBRIUM BINDING OF GALLAMINE AND *N*-[^{3}H]METHYLSCOPOLAMINE

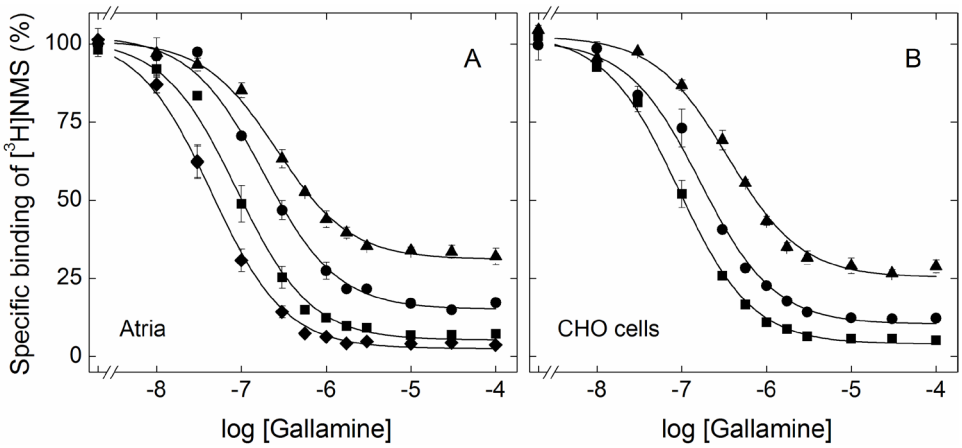

Figure S18. Inhibition of *N*-[^{3}H]methylscopolamine at low concentrations of gallamine prior to the attainment of equilibrium. Gallamine and [^{3}H]NMS were mixed simultaneously with membranes from porcine atria (A) or CHO cells expressing the M_2 receptor (B), and total binding was measured after incubation of the reaction mixture at 24 °C for 3 h. The data shown in the figure are the mean estimates of specific binding from panels A and D of Figure 5, taking only those values at lower concentrations of gallamine (*i.e.*, ≤ 0.1 mM). The concentrations of [^{3}H]NMS and the corresponding levels of occupancy in the absence of gallamine were as follows: 0.1 nM, 51.7% (♦); 0.3 nM, 76.4% (■); 1 nM, 91.5% (●); 3 nM, 97% (▲). The lines represent best fits of Equation S15, which corresponds to Scheme 2 for a system at thermodynamic equilibrium. The variables [L] and [A] are the concentrations of [^{3}H]NMS and gallamine, respectively, and K_L and K_A are the corresponding dissociation constants for binding to the vacant receptor (*i.e.*, Equations S1 and S2); α is the cooperativity factor for the effect of L on the affinity of A and *vice versa*. The variable B_{sp} represents specific binding, and $B_{sp,[A]=0}$ is specific binding in the absence of gallamine. The ratio $B_{sp}/B_{sp,[A]=0}$ is plotted on the ordinate, normalized to the mean value taken as 100. The fitted parametric values are listed in Table S16.

$$\frac{B_{sp}}{B_{sp,[A]=0}} = \frac{\left(1+\frac{[L]}{K_L}\right)\left(1+\frac{[A]}{\alpha K_A}\right)}{1+\frac{[A]}{K_A}+\frac{[L]}{K_L}\left(1+\frac{[A]}{\alpha K_A}\right)} \qquad \text{(S15)}$$

Table S16. Parametric Values for the Inhibition of *N*-[^{3}H]Methylscopolamine at Low Concentrations of Gallamine[a]

[[^{3}H]NMS]	porcine atria			CHO cells		
(nM)	log K_A	log α	α	log K_A	log α	α
0.10	−7.65 ± 0.02	−1.91 ± 0.11	0.012	—	—	—
0.30	−7.64 ± 0.05	−1.87 ± 0.11	0.014	−7.63 ± 0.02	−2.00 ± 0.07	0.010
1.0	−7.72 ± 0.05	−1.81 ± 0.05	0.015	−7.78 ± 0.05	−1.99 ± 0.06	0.010
3.0	−7.92 ± 0.03	−1.85 ± 0.02	0.014	−7.83 ± 0.05	−1.98 ± 0.03	0.011

[a] The data shown in Figure S18 were analyzed in terms of Equation S15 to obtain the parametric values listed in the table. Data at each concentration of [^{3}H]NMS were analyzed separately.

REFERENCES

1. Goodwin, J. A., Hulme, E. C., Langmead, C. J., and Tehan, B. G. (2007) Roof and floor of the muscarinic binding pocket: variations in the binding modes of orthosteric ligands. *Mol. Pharmacol. 72*, 1484–1496.

2. Haga, K., Kruse, A. C., Asada, H., Yurugi-Kobayashi, T., Shiroishi, M., Zhang, C., Weis, W. I., Okada, T., Kobilka, B. K., Haga, T., and Kobayashi, T. (2012) Structure of the human M_2 muscarinic acetylcholine receptor bound to an antagonist. *Nature 482*, 547–551.

3. Huang, X. P., Prilla, S., Mohr, K., and Ellis, J. (2005) Critical amino acid residues of the common allosteric site on the M_2 muscarinic acetylcholine receptor: More similarities than differences between the structurally divergent agents gallamine and bis(ammonio) alkane-type hexamethylene-bis[dimethyl-(3-phthalimidopropyl)ammonium]dibromide. *Mol. Pharmacol. 68*, 769–778.

4. Wells, J. W. (1992) Analysis and interpretation of binding at equilibrium. In *Receptor-Ligand Interactions. A Practical Approach.* (Hulme, E. C., Ed.) pp 289–395, Oxford University Press, Oxford.

5. Shampine, L. F. and Reichelt, M. W. (1997) The Matlab Ode Suite. *SIAM 18*, 1–22.

6. Proska, J. and Tucek, S. (1994) Mechanisms of steric and cooperative actions of alcuronium on cardiac muscarinic acetylcholine receptors. *Mol. Pharmacol. 45*, 709–717.

7. Shoup, D., Lipari, G., and Szabo, A. (1981) Diffusion-controlled bimolecular reaction rates. The effect of rotational diffusion and orientation constraints. *Biophys. J. 36*, 697–714.

8. Tränkle, C., Weyand, O., Voigtländer, U., Mynett, A., Lazareno, S., Birdsall, N. J. M., and Mohr, K. (2003) Interactions of orthosteric and allosteric ligands with [^{3}H]dimethyl-W84 at the common allosteric site of muscarinic M_2 receptors. *Mol. Pharmacol. 64*, 180–190.

9. Tränkle, C., Weyand, O., Schroter, A., and Mohr, K. (1999) Using a radioalloster to test predictions of the cooperativity model for gallamine binding to the allosteric site of muscarinic acetylcholine M_2 receptors. *Mol. Pharmacol. 56*, 962–965.